The Ballast Effect of Lithogenic Matter and its Influences on the Carbon Fluxes in the Indian Ocean

Tim Rixen[1,2], Birgit Gaye[2], Kay-Christian Emeis[2,3], Venkitasubramani Ramaswamy[4]

5 [1]Leibniz Center for Tropical Marine Research, Bremen, 28359, Germany
[2]Institute of Geology, University of Hamburg, Hamburg, 20146, Germany
[3]Helmholtz-Zentrum Geesthacht, Institute of Coastal Research, Geesthacht, 21502, Germany
[4]National Institute of Oceanography, Dona Paula, Goa, 403004, India

Correspondence to: Tim Rixen (Tim.Rixen@leibniz-zmt.de)

10 **Abstract.** Data obtained from long-term sediment trap experiments in the Indian Ocean were analysed in conjunction with satellite-derived observations and results obtained from a box model to study the influence of primary production and the ballast effect on organic carbon flux into the deep sea. The results are used to better understand the associated impacts on the CO_2 uptake of the organic carbon pump. In line with other findings derived from global data sets, our results suggest that a preferential export of organic matter in slower-sinking particles reduces the transfer efficiency of exported organic matter in

15 high-productive systems compared with low-productive regions. The resulting enhanced respiration of organic matter maintains the high nutrient availability in the surface ocean and thus the high productivity during the summer and winter bloom in the Arabian Sea. In turn, mineral ballast is essential for the transport of organic matter and nutrients into the deep sea. The additional lithogenic ballast effect can increase organic carbon fluxes by 60 %. Our model results indicate that lithogenic ballast enhances the CO_2 uptake of the organic carbon pump by increasing the amount of nutrients utilised by the

20 organic carbon pump to bind CO_2. By enhancing the export of organic matter into the deep sea, the ballast effect increases the residence time of these nutrients in the ocean. They lose the attached CO_2 if they are introduced into the surface ocean at higher latitude, where the lack of light prevents photosynthesis in winter. Considering the impact of the lithogenic ballast effect on the organic carbon export into the deep sea and the enhanced mobilisation of lithogenic matter due to land-use changes, it is assumed that humans influence the CO_2 uptake of the organic carbon pump, which might hold relevance for the

25 discussion about the anthropogenic CO_2 uptake of the ocean.

1 Introduction

Photosynthesis and the export of organic matter from the euphotic zone into the deep sea drives the organic carbon pump and is an integral part of the global carbon cycle (Volk and Hoffert, 1985). The amount of nutrients used to fix CO_2 strongly influences the CO_2 uptake of the organic carbon pump. At present, phytoplankton utilises about half of the nutrients stored in

30 the ocean. The other half eludes its utilisation and remains biologically unused (Knox and McElroy, 1984; Sarmiento and

Toggweiler, 1984; Siegenthaler and Wenk, 1984). These nutrients are called preformed nutrients (Broecker et al., 1985) and they separate from the biologically-used nutrient pool. At higher latitudes, preformed nutrients form as upwelling and convective mixing induce nutrients and CO_2 released during the respiration of formerly-exported organic matter into the surface layer and the lack of light prevents their utilisation in winter. CO_2 can return into the atmosphere and convective

5   mixing and subduction of denser polar water beneath the warmer and lighter subtropical water masses restore the detached and biologically-unused preformed nutrients into the deep ocean. The lower the preformed nutrient concentration, the more CO_2 that can be stored by the organic carbon pump (e.g. Ito and Follows, 2005).

The ballast effect is another process that – in addition to the formation of preformed nutrients – affects the CO_2 uptake of the organic carbon pump because it influences the water depth at which the exported organic matter respires (e.g. Haake and

10   Ittekkot, 1990; Ittekkot, 1993; Kwon et al., 2009). If organic matter respires within the euphotic zone, the released CO_2 can immediately return into the atmosphere. If it respires in the deep sea, CO_2 and nutrients are injected into the ocean's long-term overturning circulation, where they can be stored about 1,500 years (De La Rocha and Passow, 2014; Heinze et al., 1991). Organic matter – which reaches the surface sediments and becomes buried – detracts CO_2 from the climate system over geological times. The ballast effect increases the organic carbon flux into the deep sea by lowering its respiration in the

15   water column mainly due to two processes: minerals, which cause the ballast effect can (i) adsorb and/or integrate organic molecules onto and into their structure (Armstrong et al., 2002) and (ii) increase the sinking speed (Haake and Ittekkot, 1990; Hamm, 2002; Ramaswamy et al., 1991). The former protects organic matter against bacterial attacks and the latter reduces the time of respiration in the water column. Carbonates, biogenic opal and lithogenic matter are the main ballast minerals. Marine plankton produces carbonates and biogenic opal, whereas lithogenic matter is formed during the

20   weathering of rocks on land. Its input as dust and by rivers into the ocean is thus a steering mechanism linking the CO_2 uptake of the organic carbon pump directly to processes on land (Ittekkot and Haake, 1990).

Results obtained from sediment trap experiments in the northern Indian Ocean have indicated that aeolian dust inputs (Haake and Ittekkot, 1990) and lithogenic matter discharges from rivers mainly drive the ballast effect in the Arabia Sea and the Bay of Bengal, respectively (Ittekkot, 1993; Ittekkot and Haake, 1990). Due to a stronger ballast effect in the river-dominated

25   system, an enhanced share of the organic matter exported from the euphotic zone (export production) reached the deep sea in the Bay of Bengal (Rao et al., 1994). The Asian monsoon and its influence on the nutrient supply into the euphotic zone was in turn suggested to control primary and export production in both basins (Haake et al., 1993; Ittekkot et al., 1991; Nair et al., 1989; Rixen et al., 1996; Rixen et al., 2009). The combined impact of primary production and the ballast effect on the organic carbon export into the deep sea has not yet been studied in detail and the ballast effect has also not been quantified.

30   However, in contrast to these findings, a Multiple Linear Regression Analysis (MLR) using a global compilation of sediment trap data including data from the Indian Ocean showed that primary production hardly affects organic carbon fluxes and that carbonate is the main ballast mineral controlling the organic carbon export into the deep sea in the world's ocean (Klaas and Archer, 2002). This result was supported by Francoise et al. (2002) suggesting that in addition to the carbonate ballast, the recycling of organic matter in the surface ocean influences the organic carbon flux into the deep sea. This is believed to play

an important role in diatom-dominated systems where lower recycling efficiency and the associated reduced transfer of organic matter to higher trophic levels favours the export of more labile organic matter and lowers the formation of fast-sinking zooplankton faecal pellets. Consequences include an enhanced export of labile organic matter in slower-sinking aggregates, which increases the respiration in the water column and reduces the organic carbon flux into the deep sea. The

5   contribution of lithogenic matter was in turn assumed to be too low to significantly contribute to the ballast effect, aside from in near-shore environments. However, recent sediment trap experiments have emphasised the role of Saharan dust inputs and lithogenic matter as ballast mineral for the organic carbon export even in the subtropical gyre of the North Atlantic Ocean, where fluxes are among the lowest measured worldwide (Pabortsava et al., 2017).

Based on an expanded global compilation of sediment trap data, a geographical weighted analysis identified carbonate and

10   lithogenic matter as the main ballast minerals in the Arabian Sea and the Bay of Bengals (Wilson et al., 2012), whereas an MLR applied to data from the Indian Ocean emphasised the role of biogenic opal as the main ballast mineral (Ragueneau et al., 2006). Considering the origin of potential ballast minerals, it is crucial to know which mineral acts when and where to better understand the response of the organic carbon pump to global change. Despite its potential to respond to global changes (e.g. DeVries and Deutsch, 2014; Duce et al., 2008; Laufkötter et al., 2017; Riebesell et al., 2007), there are strong

15   uncertainties about the magnitude and direction of change (Passow and Carlson, 2012) and its role is largely neglected in the discussion about the anthropogenic CO_2 uptake of the ocean (Sabine and Tanhua, 2009). If carbonate and/or biogenic opal act as the main ballast minerals, changes of marine ecosystems can affect the ballast effect, whereas if lithogenic matter are the main ballast, human-induced land-use changes can influence it via their impact on weathering and erosion on land.

Annual means obtained from our sediment trap experiments contributed ca. 30% to the global data set used by Wilson et al.

20   (2012), although some of our data were still missing in the global compilation. Here, we compiled all of our sediment trap results (Fig. 1, Tab. 1) and analysed them in conjunction with satellite data to study the influence of the monsoon-driven primary and export production as well as the impact of individual ballast minerals on the organic carbon fluxes into the deep Indian Ocean. Furthermore, we produced a discrete-time box model to investigate impacts of the ballast effect on the CO_2 uptake of the organic carbon pump in the ocean.

25   **2. Study Area**

The Asian monsoon strongly influences the northern Indian Ocean with its two semi-enclosed basins: the Arabian Sea and the Bay of Bengal. The sea-level pressure difference between the Asian landmass and the Indian Ocean drives the monsoon (Ramage, 1987, 1971). Following the pressure gradient and deflected by the Coriolis force, the wind blows from the NE over the Arabian Sea and the Bay of Bengal between December and February (NE monsoon, Currie et al., 1973). In summer

30   (June - September), the situation reverses. The heating of the Asian landmass leads to the formation of a strong atmospheric low, which diverts the Inter Tropical Convergence Zone (ITCZ) northwards. The SE trade winds cross the equator and blow from the SW over the Arabian Sea due to the associated change of the Coriolis force. This results in the development of a

strong low-level jet (Findlater Jet), as indicated by enhanced wind speeds over the Arabian Sea (Fig. 2a,b, Findlater, 1969; Findlater, 1977).

In the Arabian Sea, the positive wind stress curl west of the axis of the Findlater Jet causes upwelling, which is strongest along the coast of the Arabian Peninsula, as indicated by low sea surface temperatures (Fig. 3, Bauer et al., 1991; Luther and

5 O'Brien, 1990; Ryther and Menzel, 1965; Sastry and D'Souza, 1972). Weaker upwelling systems also occur NE off Sri Lanka (SD) and along the SW coast of India (Sharma, 1978; Shetye et al., 1990; Wiggert et al., 2006), whose signals are carried by the Southwest Monsoon Current (SMC) into the southern Bay of Bengal (Unger et al., 2003). Contrary to the Atlantic and Pacific Oceans, where major eastern boundary upwelling systems develop, the only larger upwelling system in the eastern Indian Ocean emerges off South Java and Bali during the boreal summer (Susanto et al., 2001).

10 During their passage over the Indian Ocean, the monsoon winds gather water vapour sustaining the heavy rainfall over the Indian subcontinent and the Indonesian Archipelago (Ramesh Kumar and Prasad, 1997; Ramesh Kumar and Schlüssel, 1998). The monsoon rains feed one of the world's largest river systems (Ganges-Brahamaputra-Meghna), which originates in the Himalayas and has its maximum discharge into the Bay of Bengal in summer (Ludwig et al., 1996; Milliman and Meade, 1983; Milliman et al., 1984; Subramanian et al., 1985). Unlike the Indian subcontinent, Indonesia has no major

15 rivers because it comprises relatively small islands. Nevertheless, model studies suggest that the small Indonesian rivers contribute ~11% ($4.26 * 10^{12}$ m^{3}yr^{-1}) to the global freshwater discharge into the ocean (Syvitski et al., 2005). This exceeds river discharges from the Ganges-Brahmaputra-Meghna ($1.3 * 10^{12}$ m^{3}yr^{-1}) and the three largest rivers draining into the Arabian Sea: Indus (< 0.09 10^{12} m^{3}yr^{-1}), Narmada (< 0.04 10^{12} m^{3}yr^{-1}) and Tapti (< 0.009 10^{12} m^{3}yr^{-1}) (Milliman and Farnsworth, 2011). Due to the high freshwater water inputs, low salinity surface waters (salinity < 33) fringe the continental

20 shelves and margins in the eastern Indian Ocean north of the equator and the high salinity waters (salinity > 35) reflect the negative freshwater balance in the Arabian Sea (Fig. 2c,d).

The inputs of suspended sediments from the Ganges-Brahmaputra-Meghna (1060 Mt yr^{-1}) and Indonesian rivers (1630 Mt yr^{-1}) represent 80% and 20% of the suspended sediment inputs into the Indian and the world's ocean (Milliman and Farnsworth, 2011; Syvitski et al., 2005). About 42% of the Ganges-Brahmaputra-Meghna sediment load accumulates in the

25 subaquatic delta and about 20% feeds the Bengal deep-sea fan (Palamenghi et al., 2011 and references therein). The Bengal fan is the world's largest deep-sea fan and covers almost the entire Bay of Bengal. Estimates of the organic carbon burial rate in the Bengal fan vary between 7.2 and 13.2 Tg C yr^{-1} (France-Lanord and Derry, 1997; Galy et al., 2007). Considering that only half of organic matter is produced by marine plankton and the other half is supplied from land (Galy et al., 2007), the organic carbon burial in the fan represents 40% of the global deep sea organic carbon sedimentation. Estimates of the global

30 deep sea organic carbon sedimentation range between 8 and 17 Tg C yr^{-1} (Cartapanis et al., 2016; Jahnke, 1996).

Due to the numerous small rivers and the deep trench off Java and Sumatera, no deep-sea fan comparable to those in the Bay of Bengal is known from the Indonesian seas. At present, the sediment discharge from the Indus only amounts to about 10 Mt yr^{-1} (Milliman and Farnsworth, 2011) and is largely trapped at the Indian continental shelf and margin due to the prevailing current regime (Ramaswamy et al., 1991). In the western part of the basin, where the formation of High Salinity

Arabian Sea Water (Rochford, 1966; Tchernia, 1980; Tegen and Fung, 1995) shows negligible freshwater inputs (Fig. 2 c,d), eolian dust inputs are the main sources of lithogenic matter (Clemens et al., 1991; Sirocko et al., 1993; Tegen and Fung, 1995).

3. Methods

3.1 Sediment Trap Data

Our sediment trap experiment started in 1986 and was expanded into the Bay of Bengal one year later in 1987. The fieldwork ended around 1998. It was reinitiated in 2007 and 2008, although this could not be followed up due to piracy, which became an issue in the region at that time. The sediment trap sites in the northern and central Bay of Bengal were shifted slightly southward in some years, whereby the stations NBBT and CBBT were spilt into northern (NBBT-N, CBBT-N) and southern sites (NBBT-S, CBBT-S, Fig. 1, Tab. 1). The sediment trap moorings equipped with Mark 6 and 7 time-series sediment traps were deployed for periods of six months to one year with sampling intervals of mostly around 21 days. Haake et al. (1993) and Rixen et al. (1996) describe the sample processing and the analysis of the bulk components (organic carbon, carbonate, biogenic opal and lithogenic matter) in detail. Organic carbon (POC) multiplied by 1.8 results in organic matter (OM). The lithogenic matter flux represents the difference between the total flux and fluxes of OM, carbonate and biogenic opal.

The accuracy of sediment trap measurements is biased by a variety of hydrodynamic, biological and chemical processes (Antia, 2005; Buesseler et al., 2007; e.g., Gust et al., 1992; Gust et al., 1994; Lee et al., 1992). Since current velocities and resulting hydrodynamic effects decrease with depth and zooplankton migration is restricted to a water depth of < 600 – 900 m, particle fluxes measured at a water depth of > 1500 m are considered as the terminal gravitational transport (Bianchi et al., 2013; Honjo et al., 2008). Nevertheless, studies using radiochemical tracers suggest a trapping efficiency of deep-moored sediment traps of 98 ± 13% (Honjo et al., 2008 and references therein).

Due to logistical constrains, we were able to measure particle fluxes for more than 150 days year^{-1} over a period of seven and more years only at four sites (Tab. 2). Two of them were in the Arabian Sea (WAST and EAST) and two were in the Bay of Bengal (NBBT-N and SBBT). At these sites, the interannual variability of the annual mean particle fluxes was < ±17%. Since this resembles the error range potentially caused by the trapping efficiency, we ignored the interannual variability and focus on monthly, seasonal and annual means in this study (Tab. 3). The considered seasons are summer (June - September), winter (January - April) and inter-monsoon periods (May and October to December). In order to calculate these means, all data measured during the respective seasons were considered, including those measured e.g. at WAST in 2007 and 2008 as well as those measured at NEAST during the winter monsoon season in 2007/08. Since the trap at EPT in the northern Arabian Sea was deployed at a water depth of 590 m (Tab. 1), the EPT data were excluded from the analysis as well as data measured at NAST, WPT, where the records did not cover a full season.

3.2 Satellite Data

Monthly mean wind speeds and salinity data were derived from the Scatterometer Climatology of Ocean Winds (Risien and Chelton, 2008) and the Soil Moisture and Ocean Salinity (SMOS) satellite mission, respectively. The SMOS data covering the period between 2010 and 2012 were downloaded from ftp://ftp.icdc.zmaw.de/smos_sss/. The monthly mean satellite-derived sea surface temperatures (SST, Smith et al., 2008) were obtained from

5   ftp://ftp.emc.ncep.noaa.gov/cmb/sst/oimonth_v2/ASCII_UPDATE. Primary production rates (PP) derived from the Vertically Generalized Production Model (VGPM, Behrenfeld and Falkowski, 1997) were downloaded from http://www.science.oregonstate.edu/ocean.productivity and averaged as the SST data at around 1 degree around the trap location.

Equations 1 - 3 introduced by Eppley and Peterson (1979), Law et al. (2000) and Henson et al. (2011) were used to convert

10   primary into export production ($POC_{euphotic}$).

$$E: POC_{euphotic\ zone} = {0.0025 \cdot PP^2 \to PP < 200 \atop 0.5 \cdot PP \to PP > 200} \tag{1}$$

$$L: POC_{euphotic\ zone} = (-0.02 \cdot SST + 0.63) \cdot PP \tag{2}$$

$$H: POC_{euphotic\ zone} = 0.23 \cdot exp^{(-0.08 \cdot SST)} \cdot PP \tag{3}$$

Eppley and Peterson (1979) suggested two different equations for PP < and > 200 g m^{-2} year^{-1}. The monthly mean primary and export production rates converging the period between 2002 and 2015 were used to calculate long-term monthly, seasonal and annual means, which were linked to the averaged sediment trap data (Fig. 4). The data from the sediment trap study off South Java (JAM) overlap with the time-series observation of primary production (Fig. 5).

3.3 Multiple Linear Regression Analysis (MLR)

Similar to other studies (e.g. Klaas and Archer, 2002; Ragueneau et al., 2006; Wilson et al., 2012), a Multiple Linear Regression Analysis was applied to calculate carrying coefficients (f). Here, we used the OLS regression analysis included in the Phyton module statsmodels:

$$F_{POC} = (f_{Lith.} \cdot F_{Lith.}) + (f_{Opal} \cdot F_{Opal}) + (f_{Carb.} \cdot F_{Carb.}) \tag{4}$$

(F) represents fluxes of respective bulk components lithogenic matter (Lith.), biogenic opal (Opal) and carbonate (Carb.). In order to estimate the relative importance of individual ballast minerals (RIB) for the POC flux (F_{POC}), their contribution to

30   the predicted POC flux was calculated.

$$RIB_i[\%] = \frac{100}{F_{POC}} \cdot (f_i \cdot F_i) \tag{5}$$

(i) indicates the different ballast minerals.

3.4 Sinking Speed

In addition to statistical methods, the influence of the individual ballast minerals can also be derived from a more
5 mechanistic approach by quantifying their contribution to the density of the solids (ρ_{solids}):

$$\rho_{solids} = \frac{(Lith\% \cdot D_{lith}) + (OM\% \cdot D_{OM}) + (Opal\% \cdot D_{Opal}) + (Carb.\% \cdot D_{Carb.})}{100} \qquad (6)$$

Lith%, OM%, Opal% and Carb% are the percentage of the respective ballast minerals in the sinking particles collected in the
10 sediment traps and (D) represents their density (Tab. 4). The density of solids is the term describing the effect of mineral
particles on the sinking speed of particles within Stoke's law. Stoke's law derived from the Navier-Stoke equation is a
commonly-used parameterisation for calculating the sinking velocity (U) of particles (e.g., Engel et al., 2009; Lal and
Lerman, 1975; McCave, 1975; Miklasz and Denny, 2010):

15 $$U = \frac{(2 \cdot g \cdot \Delta\rho \cdot radius^2)}{9\eta} \qquad (7)$$

(g) is the gravitational acceleration and (radius) defines the radius of the sinking particle. (η) is the viscosity and ($\Delta\rho$)
represents the excess density of particles over water or – expressed in other words – the difference between the density of the
particle ($\rho_{particle}$) and sea water ($\rho_{seawater}$).

$$\Delta\rho = \rho_{particle} - \rho_{seawater} \qquad (8)$$

The density of a particle results from its pore water content and the density of the solids:

25 $$\rho_{particle} = (porosity \cdot \rho_{water}) + (1 - porosity) \cdot \rho_{solids} \qquad (9)$$

This equation indicates that an increasing (ρ_{solids}) enhances ($\rho_{particle}$) and thus $\Delta\rho$ (Eq.8), and finally the sinking speed (U,
Eq.7). In turn, the calculated sinking speed (U) can be used to estimate the organic carbon fluxes (POC) at the trap depth (z)
according to equation 10 introduced by Banse (1990):

$$POC(z) = POC_{euphotic} \cdot e^{\left[\frac{-\lambda \cdot (z - depth\,of\,the\,euphotic\,zone)}{sinking\,speed}\right]} \qquad (10)$$

λ) is the POC-specific respiration rate and (POC$_{euphotic}$) is the export production, which in our case was obtained by applying Eqs. 1 - 3 to the satellite-derived primary production rates.

The reliability of the calculated sinking speeds (U) and the export production rates (POC$_{euphotic}$) can be estimated by comparing the calculated organic carbon fluxes POC(z) with those measured at the sediment trap sites. This will be

5   discussed in Chapter 4.3. Since we were interested in the influence of ballast minerals on the sinking speeds, the densities were varied and other parameters required to calculate sinking speeds and organic carbon fluxes were kept constant (Tab. 4). We searched the literature to select the most realistic values for the constants to calculate sinking speeds and the organic carbon fluxes.

(λ) was assumed to vary in a relatively narrow range (0.106 ± 0.028 day^{-1} (Iversen and Ploug, 2010; Ploug and Grossart,

10   2000), whereas more recent studies suggest that λ decreases with decreasing temperatures (Iversen and Ploug, 2013; Marsay et al., 2015). Direct field observations are scarce (Laufkötter et al., 2017) but *in-situ* incubation experiments carried out at a water depth of < 500 m indicate respiration rates of 0.4 ± 0.1 and 0.01± 0.02 day^{-1} in the subtropical North Atlantic Ocean and the Southern Ocean, respectively (McDonnell et al., 2015). We selected a λ of 0.106 day^{-1}, which is well within this range.

15   The viscosity of the fluid (η) and the density of sea water (ρ$_{water}$) can be calculated as a function of sea water temperature and salinity (Millero and Poisson, 1981; Wagner and Pruß, 2002). We used a temperature and salinity of 10°C and 35 to calculate these parameters. At our sediment trap sites, the porosity of particles and the radius are unknown. Based on results derived from other studies, we selected a porosity of 0.917 (Logan and Hunt, 1987).

The equivalent spherical diameters (ESD) of sinking particles cover a wide size spectrum ranging mostly between 0.01 and <

20   5 mm (Guidi et al., 2009; Iversen et al., 2010). Particles formed in the rolling tanks often exceed 1 mm, reached ESDs of > 1 cm and resemble in size marine snow collected by scuba divers in the surface water of the ocean revealing ESDs of up to 7.5 cm (Alldredge and Gotschalk, 1988; Engel et al., 2009). An ESD of 0.1 mm is a commonly-considered threshold dividing small and large particles (Durkin et al., 2015; Guidi et al., 2009). We selected an ESD of 0.15 mm to calculate sinking speeds. Therefore, our approach ignores the notion that minerals could protect organic matter (Keil and Hedges, 1993) and

25   possibly influence the radius and porosity of particles (e.g., Hamm, 2002; Iversen and Robert, 2015). Accordingly, our model is restricted to the impact of ballast minerals on the sinking speed of particles.

3.5 Box Model

A four-box model was developed comprising an atmosphere and an ocean. The ocean was subdivided into a euphotic zone

30   (e), a seasonal thermocline (s) and a deep sea (d). The marine boxes cover the depth ranges between 0 and 100 m (euphotic zone), 100 and 300 m (seasonal thermocline) and between 300 and 3690 m (deep sea). A residence time of 1 and 1,500 years was considered for calculating fluxes of water between the three ocean boxes. This results in a water flux of 3229 Sv (= 10^6 m^3 s^{-1}) and 25 Sv between the euphotic zone and the seasonal thermocline (F$_{es}$) and between the seasonal thermocline and the deep sea (F$_{sd}$), respectively.

The box model is a discrete-time model. Changes to variables are tracked in time steps of one day using a recursion of equations (Eqs. 11- 23), which describe the values of the variables in the next time unit (t+1) as a function of the variable in the current time unit (t). Variables represent concentrations of total dissolved inorganic carbon (DIC), total alkalinity (TA) and dissolved phosphate (PO_4) and the partial pressure of CO_2 (pCO_2) as well fluxes of water (F_{es} and F_{ed}) and CO_2 (F_{CO2}).

5    $rDIC_{(e,s,d)}$, $rTA_{(e,s,d)}$ and $rPO_{4(e,s,d)}$ represent reservoir sizes of the four boxes in mole DIC, TA and PO_4. POC indicates the amount of organic carbon produced by the utilisation of PO_4 in the euphotic zone. (factor) and (f) are constants determining the fraction of phosphate (PO_4) used to produce organic matter (Eq.14) and the fraction of the exported organic matter that reaches the deep sea (Eqs. 18-23). Other constants are the Redfield C/P ratio (106), the rain ratio (RR= POC/PIC= 0.7), the gas transfer coefficient (k=38.29 cm hr^{-1}), the seawater temperature (14.2°C), the salinity (34.77) and thus also the solubility

10   product of CO_2 in water (α).

Atmosphere (A)

$$pCO_{2A}(t+1) = [rCO_2(t) + F_{CO2}(t)]/2.18 \qquad (11)$$

$$F_{CO2}(t) = k \cdot \alpha \cdot (pCO_{2A}(t) - pCO_{2W}(t)) \qquad (12)$$

Euphotic zone (e)

$$pCO_{2w}(t) = Function[DIC_e(t), TA_e(t), PO_{4e}(t), Temperature_e, Salinity_e] \qquad (13)$$

$$POC(t) = (106 \cdot rPO_{4e}(t) \cdot factor) \qquad (14)$$

$$DIC_e(t+1) = \left[rDIC_e(t) + F_{es} \cdot [DIC_s(t) - DIC_e(t)] - POC(t) - \left(\frac{POC(t)}{RR}\right) - F_{CO2}(t)\right]/Vol_e \qquad (15)$$

20    $$TA_e(t+1) = \left[rTA_e(t) + F_{es} \cdot [TA_s(t) - TA_e(t)] + 0.15 \cdot POC(t) - 2 \cdot \left(\frac{POC(t)}{RR}\right)\right]/Vol_e \qquad (16)$$

$$PO_{4e}(t+1) = \left[rPO_{4e}(t) + F_{es} \cdot [PO_{4s}(t) - PO_{4e}(t)] - \left(\frac{POC(t)}{106}\right)\right]/Vol_e \qquad (17)$$

Seasonal thermocline (s)

$$DIC_s(t+1) = \left[rDIC_s(t) + F_{es} \cdot [DIC_e(t) - DIC_s(t)] + F_{sd} \cdot [DIC_d(t) - DIC_s(t)] + (1-f) \cdot POC(t) + (1-f) \cdot \left(\frac{POC(t)}{RR}\right)\right]/Vol_s \qquad (18)$$

25    $$TA_s(t+1) = \left[rTA_s(t) + F_{es} \cdot [TA_e(t) - TA_s(t)] + F_{sd} \cdot [TA_d(t) - TA_s(t)] - (1-f) \cdot 0.15 \cdot POC(t) + (1-f) \cdot 2 \cdot \left(\frac{POC(t)}{RR}\right)\right]/Vol_s \qquad (19)$$

$$PO_{4s}(t+1) = \left[rPO_{4s}(t) + F_{es} \cdot [PO_{4e}(t) - PO_{4s}(t)] + F_{sd} \cdot [PO_{4d}(t) - PO_{4s}(t)] + (1-f) \cdot \left(\frac{POC(t)}{106}\right)\right]/Vol_s \qquad (20)$$

Deep sea (d):

$$DIC_d(t+1) = \left[rDIC_d(t) + F_{sd} \cdot [DIC_s(t) - DIC_d(t)] + (f) \cdot POC(t) + (f) \cdot \left(\frac{POC(t)}{RR}\right)\right]/Vol_d \qquad (21)$$

30    $$TA_d(t+1) = \left[rTA_d(t) + F_{sd} \cdot [TA_s(t) - TA_d(t)] - (f) \cdot 0.15 \cdot POC(t) + (f) \cdot 2 \cdot \left(\frac{POC(t)}{RR}\right)\right]/Vol_d \qquad (22)$$

$$PO_{4d}(t+1) = \left[rPO_{4d}(t) + F_{sd} \cdot [PO_{4s}(t) - PO_{4d}(t)] + (f) \cdot \left(\frac{POC(t)}{106}\right)\right]/Vol_d \qquad (23)$$

Boundary conditions were set as similar as possible to those observed in the ocean and atmosphere. In the model, the mean TA, DIC and PO_4 concentrations were 2455 µmol kg^{-1}, 2205 µmol kg^{-1} and 2.1 mmol m^{-3}. The phosphate concentration almost equals the global mean given by Sarmiento and Gruber (2006), whereas the TA and DIC concentration are higher and lower, respectively (DIC: 2364 µmol kg^{-1}, TA: 2255 µmol kg^{-1}). The values given by Sarmiento and Gruber (2006) refer to

5   1990, when the mean atmospheric CO_2 concentration was 354 ppm (Keeling and Whorf, 2005). We modified the TA and DIC concentrations to meet this pCO_2 in the atmosphere.

Contrary to primary production – which can be measured by the uptake of ^{14}C labelled CO_2 (Nielsen, 1951) – there are no reliable methods to measure export production. The large range of estimates on the global mean export production (1.8 - 27.5 10^{15} g C yr^{-1}) reflects the resulting uncertainties (del Giorgio and Duarte, 2002; Honjo et al., 2008; Lutz et al., 2007). Based

10   on numerical model results and ocean colour data, global mean export production rates ranging between 5 and 10 Pg C yr^{-1} currently appear to be well accepted (Bopp et al., 2013; Siegel et al., 2014; Westberry et al., 2012). Accordingly, we used a fraction of 0.0005 to adjust organic carbon export to 10 Pg C yr^{-1} (Eq.14). The resulting unused phosphate was considered as preformed phosphate, which was distributed by physical processes (mixing) over the marine boxes.

4. Results and Discussion

15   ### 4.1 Organic Carbon Fluxes into the Deep Sea

The results obtained thus far from our sediment trap experiments show that monsoon-driven upwelling and convective mixing control the productivity and the carbon export into the deep sea by carrying nutrient-enriched subsurface water into the euphotic zone (Rixen et al., 2009). In the Arabian Sea, this leads to pronounced phytoplankton blooms (Fig. 2e,f) associated with enhanced fluxes into the deep sea during summer and winter, respectively (Fig. 4). In the Bay of Bengal,

20   monsoon rains over the Indian subcontinent and the resulting riverine nutrient and freshwater discharges additionally affect the organic carbon export into the deep sea. Near the coast, riverine nutrient inputs increase the organic carbon export (Ittekkot et al., 1991), whereas offshore nutrient-depleted freshwater forms a buoyant low salinity surface layer, which lowers nutrient inputs from subsurface waters into the euphotic zone (Kumar et al., 1996; Rixen et al., 2009). This effect reduces nutrient inputs during the mixed-layer deepening in winter, which – in contrast to the Bay of Bengal – increases

25   primary production (Fig. 2e,f) and carbon fluxes in the Arabian Sea (Fig. 4). Since in the Bay of Bengal our sediment traps were deployed in the more offshore regions, primary production and organic carbon exports into the deep sea reveal hardly any seasonality compared to the Arabian Sea. Furthermore, inputs of terrestrial organic matter were negligible at the trap sites (Unger et al., 2005).

Similar to the Arabian Sea and the southern Bay of Bengal, the organic carbon fluxes in the equatorial western Indian Ocean

30   off South Java show a monsoon-driven seasonality (Fig. 4a). Since this trap site was located closer to the coast than those in the Bay of Bengal, riverine nutrient discharges increase the organic carbon fluxes during the rainy season in winter (Rixen et al., 2006). In summer, costal upwelling off Java causes the high fluxes. However, the buoyant low salinity layer that forms

during the rainy season reduces the input of nutrient-enriched subsurface water during the following upwelling season, which strongly ties upwelling intensity to the ENSO-influenced precipitation rates over Indonesia (Rixen et al., 2006). Primary production rates off South Java are much lower than those in the upwelling influenced western Arabian Sea (Fig. 2 e, f and Fig. 4b), whereas organic carbon fluxes are higher off South Java than in the western Arabian Sea (Fig. 4 a). The

5   annual mean total flux measured at JAM is the highest that we have measured in the Indian Ocean at a water depth of > 1500 m (Tab. 3). Since the data from the sediment trap study off South Java are the only ones overlapping with the time-series observation of primary production, these two data sets could be directly compared (Fig. 5).

4.2 Java in Comparison to the Western Arabian Sea

The comparisons of satellite and sediment trap data showed that in the South Java Sea enhanced primary productions rates

10   correspond to high organic carbon fluxes during the upwelling season in summer, but enhanced fluxes did not reflect higher primary production rates during the rainy season (Fig. 4, 5). This decoupling between primary production and organic carbon fluxes during the rainy season could have various reasons. A dense cloud cover shading the Indonesian seas from space observations biases satellite observations (Hendiarti et al., 2004) and/or resuspended sediments from the shelf increases the organic carbon fluxes into the deep sea. Inputs of resuspended sediments should affect the biogeochemical characteristic of

15   the trapped material, although this could not be observed. For example, Mg/Ca as well as stable oxygen isotopic ratios of foraminifera shells collected by the trap were used to reconstruct sea water temperatures (Mohtadi et al., 2009). The reconstructed seawater temperatures correlate with satellite-derived sea surface temperatures suggesting that inputs of resuspended foraminifera shells biasing the sea surface temperature reconstruction could be ignored. Due to the vicinity to Java Island and its numerous rivers, freshwater diatoms were found in the trap, although they were low in number (Romero

20   et al., 2009). Since organic carbon-to-nitrogen ratios and stable carbon isotopic ratios of organic matter are in the range of marine plankton, impacts of resuspended sediments and terrestrial organic matter are assumed to be negligible at the trap site (Rixen et al., 2006). On the other hand, the mean contribution of lithogenic matter during the rainy season of 65% exceeds those during the upwelling season (55%), suggesting that a stronger ballast effect could have increased the fraction of organic carbon exported into the deep sea during the rainy season. The lithogenic matter content of > 55% could also explain

25   the overall high organic carbon flux off South Java compared with in the western Arabian Sea, where primary production is much higher than off South Java, but lithogenic matter content was only 14% (Tab. 3).

4.2 Primary Production and Organic Carbon Fluxes

In an attempt to further disentangle the impacts of primary production and the ballast effect on the organic carbon fluxes into

30   the deep sea, seasonal averaged organic carbon fluxes and export production rates were compared. The export production rates were derived from primary production rates by using equations 1 to 3. The ratio between the organic carbon flux and the export production defines the transfer efficiency (T_{eff}) of the exported organic carbon (Francois et al., 2002). Multiplied by 100, it represents the share of the export production rates, which is respired in the water column.

Based on annual means, Francois et al. (2002) suggest that 9.6 ±4.9% and 16±2.4% of the exported organic matter arrives at the sediment traps in the Arabian Sea and the Bay of Bengal. Using Eq.2 like Francois et al. (2002), our annual mean data suggest that 16.5 ±5% and 46.5±5% of the exported organic matter reach the traps. Varying SST only causes this difference. The SST that we obtained are approximately 0.6° higher than those used by Francois et al. (2002) and export

5 production derived from Eq.2 is extremely sensitive to temperature changes. However, these differences are almost negligible if one compares these results with the variability caused by using Eqs. 1 and 3. Export production rates derived from these equations suggest that 5±3% (Eq.1) and 72±25% (Eq.3) of the organic matter reaches the deep sea, respectively. This reflects that within the temperature range of relevance for our trap sites (26.5 – 28.5°C) the export production derived from Eq.1 is > 6 times higher than obtained from Eq.3. The ratio between the export production derived from Eq.1 and Eq.3

10 decreases with increasing primary productivity (Fig. 6). At primary production rates of > 200 g C m^{-2} year^{-1}, export production rates derived from Eq.3 represent < 7.5% of the export production rates obtained from Eq.1.

Nevertheless, independent of which equation is used to calculate export production rates, the share of the exported organic matter that reaches the deep sea tends to decrease with increasing export productions rates. This trend is most pronounced if one uses Eq.1 to calculate export production rates and can be described with a Michaelis-Menten type of equation (Fig. 7a).

15 This implies that respiration of organic matter in the water column is more efficient in high- rather than in low-productive systems. In our case, high-productive systems are mainly the summer and winter blooms in the Arabian Sea (Fig. 2e,f). During these phases, diatoms dominate the phytoplankton community (Garrison et al., 1998; Garrison et al., 2000), which supports the results obtained by Francois et al. (2002), suggesting that an enhanced export of labile organic matter in slower-sinking aggregates increases the respiration in the water column in high-productive diatom-dominated systems.

20 The trend line describing the respiration of organic matter in the water column as a function of export production (Fig. 7a) can be used to calculate organic carbon fluxes in the deep sea in addition to the export production rates. The difference between calculated and measured fluxes defines the excess organic carbon flux (POC_{Excess}). Independent of which equation is used to calculate export production, the resulting POC_{Excess} correlates with the lithogenic matter content, which is again most pronounced if one uses Eq.1 to calculate export production (Fig. 7b). An increasing lithogenic matter content enhances not

25 only the POC_{Excess} flux but also its contribution of the total organic carbon flux, which reaches up to 60% at JAM off South Java.

The data measured at WAST and SBBT during the upwelling season are exceptions, but instead of correlating with the lithogenic matter content, their POC_{Excess} fluxes correlate with the carbonate flux (Fig. 7b). This also holds true for data obtained at other stations, although in this case data measured in central and northern Bay of Bengal as well as the South

30 Java Sea are the exceptions (Fig. 7c). Since lithogenic matter contents of > 25% characterise these sites (Tab. 3), it is assumed that lithogenic matter acts as the main ballast material if its content increases above this threshold. In turn, carbonate seem to gain more importance if the lithogenic matter content decreases and it seems to become a dominant driver of organic carbon export in upwelling systems of the western Arabian Sea and the southern Bay of Bengal. In order to further validate this result, we applied the MLR to our data.

4.3. Carbonate versus Lithogenic Ballast

Applied to our annual means, the MLR shows that the highest carrying coefficients are associated with biogenic opal followed by those of carbonate (Tab. 5 - A-Traps). This matches the results obtained by (Ragueneau et al., 2006) and

5   disagrees with those obtained from the geographical weighted analyses, which – as previously mentioned – identified carbonate and lithogenic matter as the main ballast minerals in the Arabian Sea and the Bay of Bengals (Wilson et al., 2012).
In order to investigate regional differences within the Indian Ocean, we also applied the MLR to the data obtained by analysing the bulk composition of sinking particles collected in the individual sampling cups at each sediment trap site (Tab.
5). On average, this revealed the highest carrying coefficient in association with lithogenic matter. Weighted by multiplying

10   the carrying coefficients with the associated flux (RIB) indicates that on average lithogenic matter ballast contributes 43 ±19% to the predicted organic carbon fluxes (Tab. 6). This varies regionally and in line with our previous results carbonate was identified as the main ballast mineral at WAST. In contrast to our previous results, carbonate is also suggested as the main ballast mineral at JAM off South Java, which is surprising considering the low carbonate (10.7 %) and the high content of litghogenic matter (61.1%) in samples from these sites (Tab. 3).

15   In order to further analyse the role of carbonate and lithogenic matter as ballast mineral, we also integrated data from the U.S. JGOFS sediment trap program into our analysis. During the US JGOFS program in 1994/95, six additional sediment
traps were deployed at a water depth of > 2220 m in the western Arabian Sea off Oman (Fig. 1, Honjo et al., 1999). The annual mean lithogenic matter content obtained from the joint data set correlates with the respective organic carbon fluxes (Fig. 8 a). Exceptions are again data obtained from the high-productive upwelling-dominated western Arabian Sea. At these

20   sites, organic carbon fluxes correlate with the carbonate flux. This supports our previous results implying that the lithogenic matter ballast effect increases with increasing lithogenic matter content, whereas in regions with low lithogenic matter supply or very high productivity such as in upwelling systems carbonate exerts a dominant control on the organic carbon export.

However, Eq.6 indicates that the carbonate content rather than the carbonate flux increases the density of solids and thus the

25   sinking speed of particles. This might imply that instead of the enhanced sinking speed, the protection of organic matter against bacterial attacks – as suggested by Armstrong et al. (2000) – is the decisive processes explaining the correlation between carbonate and organic carbon fluxes. Alternatively, the correlation could also be a consequence of a joint production. This is obvious in blooms dominated by coccolithophorids, as well as those dominated by non-calcifying phytoplankton when e.g. calcifying grazers such as pelagic foraminifera prevail. In the western Arabian Sea, peak fluxes of

30   pelagic foraminifera coincide with upwelling-driven diatom blooms (Haake et al., 1993). Global tests of foraminifera are assumed to contribute 50% to the carbonate flux (Schiebel, 2002). Furthermore, they sink by their own and reveal sinking speeds of several hundred-metre day[-1] (Schiebel, 2002; Schiebel and Hemleben, 2005; Schmidt et al., 2014). Therefore, they are as fast or even faster than faecal pellets produced by copepods, which are also among the main grazers within the

upwelling system (Smith 2005; Smith, 1982; Turner, 2015). Accordingly, the correlation between organic carbon and carbonate fluxes might simply be due to the dependence of both on the productivity.

Lithogenic matter mainly comprises clay and some other minerals such as quartz with a grain of < 2µm. According to Stoke's law, such tiny mineral grains are too small to sink and should remain as suspended solids in the water column

5   (McCave, 1975). They reach the deep sea and underlying sediments incorporated into marine snow and faecal pellets (Avnimelech et al., 1982; Honjo, 1976, 1982; Kranck, 1973; McCave, 1984, 1975; Rex and Goldberg, 1958).

In contrast to carbonate, their export into the deep sea is strongly tied to the formation of sinking particles and the production of organic matter cleaving the sinking particles together. However, this raises questions concerning whether the observed changes of the lithogenic matter content suffice to alter sinking speeds required to explain POC$_{Excess}$ flux.

10   **4.4 Sinking Speeds**

In order to calculate the density of the solids (ρ_{solids}) and the sinking speed of particles, the densities of bulk components were compiled from the literature. They showed a wide range and fall below those of their crystalline analogues (Fig. 9). For example, the density of proteins varies between 1.22 to 1.47 g cm^{-3}, whereas the density of organic matter in phytoplankton comprising > 80% of amino acids varies between 1.03 and 1.1 g cm^{-3} (Lee et al., 2004; Logan and Hunt, 1987; Miklasz and

15   Denny, 2010; Quillin and Matthews, 2000). With 0.7 – 0.84 g cm^{-3}, the density of transparent exopolymers (TEP) – which play an essential role for the formation of marine snow – is even below that of seawater (Azetsu-Scott et al., 2004). Other carbohydrates such as cellulose reveal a density of 1.5 g cm^{-3}. The density of calcite – the most common calcium carbonate mineral in the pelagic ocean – is 2.71 g cm^{-3} (Mottana et al., 1978). In turn, coccolithophores and foraminifera tests reveal densities of only 1.55 g cm^{-3} (page 71, Winter and Siesser, 1994) and up to 1.7 g cm^{-3} (Schiebel et al., 2007; Schiebel and

20   Hemleben, 2000). In contrast to opal – which is a hydrous silicon oxide and reveals densities of 1.9 to 2.5 g cm^{-3} – the density of diatom frustules (biogenic opal) varies between 1.46 and 2.0 g cm^{-3} (Csögör et al., 1999; DeMaster, 2003).

The density of lithogenic matter depends on its mineral composition. Clay minerals change their density by adsorbing water, which is most pronounced within the group of smectite. Their density decreases from 2.72 to 1.4 g cm^{-3} during hydration (Osipov, 2012), whereas hydration hardly affects the density of illite, which decreases from 2.75 to 2.72 g cm^{-3}. At our trap

25   sites, illite and quartz mostly compose lithogenic matter (Ramaswamy et al., 1991; Ramaswamy et al., 1997). Since the density of quartz is 2.65 g cm^{-3}, we used a density of 2.70 ±0.05g cm^{-3} for lithogenic matter. In order to calculate the densities of the solids, we also used a density of 0.9 ±0.2, 1.73 ±0.27, and 1.63 ±0.08 for organic matter, biogenic opal and carbonate, respectively (Tab. 4).

Since lithogenic matter contributes significantly to the total flux at all of our trap sites (Tab. 3) and reveals the highest

30   density, its content largely determines the density of the solids (Fig. 10a). The mean calculated sinking speed is 203±53 m day^{-1} and falls within the range of sinking speeds (230 ±72 m day^{-1}) obtained from the US JGOFS sediment trap experiment in the Arabian Sea (Berelson, 2001). Furthermore, it agrees with the temporal delay of about 14 days between the onset of

upwelling and the associated increase of organic fluxes at water depth of about 3000 m in the Arabian Sea, suggesting a mean sinking speed of > 214 m day^{-1}(Rixen et al., 1996).

A further approach to test the validity of the obtained sinking speed is to use it to calculate organic carbon fluxes as described by Eq.4. Therefore, the required export production rates were calculated by applying Eqs. 1 - 3 to the satellite-

5   derived primary production rates, as already conducted. Independent of which equation we used, the calculated organic carbon fluxes correlate with the measured ones (Fig. 10 a,b). Nevertheless, the organic carbon fluxes obtained by using Eq.1 and 2 exceed measured fluxes, while those obtained by using Eq.3 are lower than the measured organic carbon fluxes. The calculated fluxes can be adjusted to the measured ones by changing the constant in Eq.3 from 0.23 to 0.40 (Fig. 10c).

In contrast to Eppley and Peterson (1979) – who derived Eq.1 by looking at nutrient uptake rates of phytoplankton – Henson

10   et al. (2011) obtained Eq.3 by comparing satellite-derived primary production rates with ^{234}Thorium deficits in the water column. The adsorption of ^{234}Th to sinking organic matter causes this deficit. This might imply that Eq.1 describes export production and those obtain by Henson et al. (2011) defines the export of organic matter, which reaches the deep sea. We cannot prove this hypothesis, but it agrees with the results discussed thus far and helps to explain the high productivity in the Arabian Sea.

15   The ratio between the export production derived from Eq.1 and Eq.3 decreases with increasing primary productivity, as mentioned before (Fig. 6), which indicates that in comparison to low-productive systems a reduced fraction of the exported production reaches the deep sea in high-productive regions. This implies an enhanced respiration of exported organic matter in high-productive systems as seen in our data and should increase the nutrient concentrations in the seasonal thermocline. The seasonal thermocline defines the subsurface layer from which water is introduced into the euphotic on a seasonal time

20   scale. In addition to physical nutrient supply mechanism (e.g. upwelling, winter mixing), such an enhanced nutrient trapping in shallow subsurface waters should be a factor sustaining the high productivity during the summer and winter bloom in the Arabian Sea.

As discussed before, the transfer efficiency obtained by applying Eq.3 to the satellite-derived primary production rates and comparing the resulting export production to sediment trap data was 72±25% and the sinking speeds required to explain

25   measured fluxes was about 203±53 m day^{-1}. If one assumes that Eq.1 describes the export production and Eq.3 the one which reaches the deep sea than figure 6 shows that between 6 and 15% of the organic matter is exported in the fast-sinking particles with mean speed of 203±53 m day^{-1} of which 72±25% arrives at the traps. Considering the modified Eq.3, the numbers change slightly, suggesting that an overage 15% of the exported production is exported in fast-sinking particles, of which 55% arrive in the deep sea. In turn, this implies that 85% of the exported production is exported in slow-sinking

30   particles, which never reach the trap depth. Results obtained from the Atlantic Ocean indicate that a large fraction of organic matter is exported independent from ballast minerals (Le Moigne et al., 2014). Based on our approach, sinking speeds would decrease to < 20 m day^{-1} without mineral ballast and consequently the calculated organic carbon flux into the deep would approach zero at the trap sites. Accordingly, minerals are essential for the export of organic matter into the deep sea, whereas at our trap sites lithogenic matter seems to enhance the ballast effect of the biogenic minerals.

In order to quantify the lithogenic matter ballast effect, we assumed that there is no lithogenic matter. Due to the decreasing density of the solids the sinking speed at the trap site would reduce to 146 ±61 m day⁻¹ (Fig. 10a) and the carbonate biogenic opal ratio would be the decisive factor controlling the sinking speed. On average, such a low sinking speed could decrease the calculated organic carbon fluxes at the trap sites by about 33%. At JAM in the South Java Sea, the absence of lithogenic

5   matter would even reduce the calculated organic carbon fluxes by about 60%, which almost equals the results obtained from the correlation between POC_{Excess} and the lithogenic matter content. The additional ballast effect also explains the high organic carbon fluxes favouring the high organic carbon sedimentation in the low-productive Bay of Bengal.

4.5 The Impact of the Ballast Effect on Pelagic Ecosystems the CO_2 Uptake of the Ocean

The four-box model was used to study the impact of the lithogenic matter ballast effect on the pelagic ecosystem and the

10   CO_2 uptake of the Ocean. In a first experiment, we simulated the influence of the lithogeneic ballast effect by changing the fraction of the exported organic matter that reaches the deep sea from 10 to 50% (Fig. 11-Exp. II). Due to the resulting enhanced export of organic matter into the deep sea, our box model shows – as general circulation models (Heinze et al., 1991; Kwon et al., 2009) – decreasing atmospheric CO_2 concentrations due to an enhanced storage of CO_2 and nutrients (phosphate) in the deep ocean. However, the latter also reduces the export production because it lowers the nutrient

15   concentration in the seasonal thermocline. Reducing the fraction of organic matter that is exported into the deep sea has an opposite effect (Fig. 11 – Exp. III). The CO_2 concentration and the export production increase, which – as also shown in other studies (Heinze et al., 1991) – indicates that an enhanced CO_2 uptake of the organic carbon occurs at the expense of the nutrient availability in the seasonal thermocline and thus the productivity in the surface ocean.

In the next step, we assumed that phytoplankton consumes all nutrients in the surface water and exports it as organic matter

20   into the deep sea (Fig. 11- Exp. IV). Consequently, the export production increases from about 10 to 24 Pg C year⁻¹ and the CO_2 concentration in the atmosphere decreases from 354 to about 326 ppm. In accordance with many other models, this shows the effects of an enhanced utilisation of preformed nutrients on the atmospheric CO_2 concentrations (e.g. Archer et al., 2000; Ito and Follows, 2005). However, the assumption that all nutrients are used and the preformed nutrient concentration approaches zero is unrealistic and would probably cause anoxia in the real ocean. Nevertheless, such a numerical exercise its

25   quite interesting because it provides the possibility to study the influence of the ballast effect on the CO_2 uptake of the ocean in the absence of preformed nutrients (Fig. 12).

As in previous experiments II and III, we increased and decreased the fraction of organic matter that is exported into the deep sea. The consequences were a reduced and enhanced export production due to the associated changes in deep sea nutrient storage and the nutrient concentration in the seasonal thermocline. The more nutrients that are stored in the deep sea

30   the lower the nutrient concentrations in the seasonal thermocline and the lower the amount of nutrients feeding the export production. In contrast to previous experiments, this hardly affected the organic matter flux into the deep and the atmospheric CO_2 concentration even remained almost constant. The underlying mechanism is that an enhanced export of nutrients into the deep sea lowers export production and an enhanced share of a lower export production keeps the export

into the deep sea at the same level. Vice versa, a reduced export into the deep sea increases export production and a reduced share of the enhanced export production results in unchanged export of organic matter into the deep sea.

In previous experiments (Fig. 11), this effect was masked because changes in the export of organic matter into the deep sea additionally affected the preformed nutrient concentrations. The more nutrients that the organic carbon pump introduces into

5   the deep sea, the lower the preformed nutrient concentrations. The resulting increased nutrient utilisation has two effects: first, it increases the export flux into the deep sea; and second, it enhances the CO_2 uptake of the organic carbon pump and lowers the pCO_2 in the atmosphere.

If all preformed nutrients are used, these two effects disappear because the organic carbon is running at its limit (Fig.12). Assuming that each phosphate molecule is associated with 106 moles of carbon, the organic carbon pump is saturated. As

10   such a condition, the CO_2 uptake of the organic carbon pump can only be increased by raising the C/P ratio and/or the ocean's P inventory. Vice versa, this means that the ballast effect influences the atmospheric CO_2 concentrations via its impact on the preformed nutrient formation. A stronger ballast effect leads to more organic matter respiration in the deep sea and reduces the formation of preformed nutrients in the surface ocean. Thereby, more CO_2 can be taken up by the organic carbon pump.

15   Since preformed nutrient concentrations are enhanced in polar regions, the impact of the ballast effect on the CO_2 uptake of the organic carbon pump is assumed to be stronger in higher latitudes compared with tropical regions. This supports the assumption that enhanced eolian dust inputs into the southern ocean increased CO_2 uptake of the organic carbon pump during the last glacial period not only due to the associated iron fertilisation but also through its ballast effect (Falkowski et al., 1998; Ittekkot, 1993). Since rivers introduce 83% of suspended matter into the subtropical and tropical ocean (Syvitski et

20   al., 2005), the resulting lithogenic matter ballast effect seems to mainly influence the long-term storage of CO_2, as indicated by the high organic carbon burial rates in the low-productive Bay of Bengal. Considering the estimated of an up to twentyfold increase of erosion due to deforestation and the expansion of agriculture (Neil, 2014), humans must have increased the ballast effect and the CO_2 uptake of organic carbon pump over thousands of years.

25   **5. Conclusion**

The evaluation of our data in conjunction with satellite-derived observations shows – in line with other results – that the transfer efficiency of the exported organic matter is lower in high- compared with low-productive systems due to a preferential export of organic matter in slower-sinking particles. The resulting enhanced respiration of organic matter in the water column sustains (in addition to the physical nutrient supply mechanisms) the high productivity by increasing nutrient

30   trapping in shallow subsurface waters.

Biogenic mineral ballast is essential for the transport of organic matter into the deep sea, whereas at our trap sites lithogenic matter exerts an additional ballast effect, which could increase the organic carbon fluxes by up 60%. Due to the lithogenic

matter ballast effect, organic carbon fluxes in the low-productive South Java Sea exceeds those measured in the high-productive upwelling-driven western Arabian Sea. Furthermore, it increases the organic carbon fluxes in the river-dominated Bay of Bengal and favours organic carbon burial. Organic carbon burial in the Bengal deep sea fan represents approximately 40% of the global deep sea organic carbon sedimentation and thus acts as an important long-term sink of CO_2.

5 In accordance with other studies, our model results show that the ballast effect reduces the productivity by feeding nutrients into the ocean's long-term overturning circulation. This in turn extends the residence time of nutrients and the attached CO_2 in the ocean, which lowers the formation of preformed nutrients and increases the CO_2 uptake of the organic carbon pump. Since preformed nutrient concentrations are higher in polar rather tropical regions, it is assumed that the influence of the ballast effect on CO_2 uptake of the organic carbon in the ocean is stronger at higher compared with lower latitudes. However,

10 due to land-use changes and the associated enhanced mobilisation of lithogenic matter, humans have influenced the organic carbon pump over thousands of years, which today could hold relevance for the discussion about the fate of anthropogenic CO_2.

Acknowledgment

15 First of all, we would like to thank all of the scientists, technicians, officers and their crews of the numerous research vessels used during our studies in the Indian Ocean. We would specifically like to express our gratitude to the Federal German Ministry for Education, Science, Research and Technology (BMBF, Bonn ref. no. 03F0463A), the Council of Scientific and Industrial Research (CSIR, New Delhi), the Ministry of Earth Sciences (MOES, New Delhi), and the Agency for the Assessment and Application of Technology (BPPT), Jakarta, Indonesia for financial support. P. Wessels and W.H.F Smith

20 are acknowledged for providing the generic mapping tools (GMT) and we are grateful to A. Merico for helpful discussions.

References

Alldredge, A. L. and Gotschalk, C.: In situ setting behavior of marine snow, Limnology and Oceanography, 33, 339-351, 1988.
Antia, A. N.: Solubilization of particles in sediment traps: revising the stoichiometry of mixed layer export, Biogeosciences,
25 2, 189-204, 2005.
Archer, D. E., Eshel, G., Winguth, A., Broecker, W., Pierrehumbert, R., Tobis, M., and Jacob, R.: Atmospheric pCO$_2$ sensitivity to the biological pump in the ocean, Global Biogeochemical Cycles, 14, 1219-1230, 2000.
Armstrong, R. A., Lee, C., Hedges, J. I., Honjo, S., and Wakeham, S.: A new, mechanistic model for organic carbon fluxes in the ocean: based on the quantitative association of POC with ballast minerals, Deep Sea Research, 49, 219 - 236,
30 2002.
Avnimelech, Y., Troeger, B. W., and Reed, L. W.: Mutual Flocculation of Algae and Clay: Evidence and Implications, Science, 216, 63-65, 1982.
Azetsu-Scott, Kumiko, and Passow, U.: Ascending marine particles: Significance of transparent exopolymer particles (TEP) in the upper ocean, Limnology Oceanography, 49, 741 - 748, 2004.

Banse, K.: New views on the degradation and disposition of organic particles as collected by sediment traps in the open sea, Deep Sea Research, 37, 1177-1195, 1990.

Bauer, S., Hitchcock, G. L., and Olson, D. B.: Influence of monsoonally-forced Ekman dynamics upon surface layer depth and plankton biomass distribution in the Arabian Sea, Deep Sea Research, 38, 531-553, 1991.

5 Behrenfeld, M. J. and Falkowski, P. G.: Photosynthetic rates derived from satellite-based chlorophyll concentration, Limnology and Oceanography, 42, 1-20, 1997.

Berelson, W. M.: Particle settling rates increase with depth in the ocean, Deep Sea Research Part II: Topical Studies in Oceanography, 49, 237-251, 2001.

Bianchi, D., Galbraith, E. D., Carozza, D. A., Mislan, K. A. S., and Stock, C. A.: Intensification of open-ocean oxygen 10 depletion by vertically migrating animals, Nature Geosci, 6, 545-548, 2013.

Bopp, L., Resplandy, L., Orr, J. C., Doney, S. C., Dunne, J. P., Gehlen, M., Halloran, P., Heinze, C., Ilyina, T., Séférian, R., Tjiputra, J., and Vichi, M.: Multiple stressors of ocean ecosystems in the 21st century: projections with CMIP5 models, Biogeosciences, 10, 6225-6245, 2013.

Broecker, W. S., Takahashi, T., and Takahashi, T.: Sources and Flow Patterns of Deep-Ocean Waters as Deduced From 15 Potential Temperature, Salinity, and Initial Phosphate Concentration, Journal of Geophysical Research, 90, 6925-6939, 1985.

Buesseler, K. O., Antia, A. N., Chen, M., Fowler, S. W., Gardner, W. D., Gustafsson, O., Harada, K., Michaels, A. F., Rutgers van der Loeff, M., Sarin, M., Steinberg, D. K., and Trull, T.: An assessment of the use of sediment traps for estimating upper ocean particle fluxes, Journal of Marine Research,, 65, 345 - 416, 2007.

20 Cartapanis, O., Bianchi, D., Jaccard, S. L., and Galbraith, E. D.: Global pulses of organic carbon burial in deep-sea sediments during glacial maxima, Nat Commun, 7, 2016.

Clemens, S., Prell, W., Murray, D., Shimmield, G., and Weedon, G.: Forcing mechanisms of the Indian Ocean monsoon, Nature, 353, 720-725, 1991.

Csögör, Z., Melgar, D., Schmidt, K., and Posten, C.: Production and particle characterization of the frustules of Cyclotella 25 cryptica in comparison with siliceous earth, Journal of Biotechnology, 70, 71-75, 1999.

Currie, R. I., Fisher, A. E., and Hargreaves, P. M.: Arabian Sea Upwelling. In: Biology of the Indian Ocean, 1973.

De La Rocha, C. L. and Passow, U.: 8.4 - The Biological Pump. In: Treatise on Geochemistry (Second Edition), Turekian, H. D. H. K. (Ed.), Elsevier, Oxford, 2014.

del Giorgio, P. A. and Duarte, C. M.: Respiration in the open ocean, Nature, 420, 379-384, 2002.

30 DeMaster, D. J.: 7.04 - The Diagenesis of Biogenic Silica: Chemical Transformations Occurring in the Water Column, Seabed, and Crust A2 - Turekian, Heinrich D. HollandKarl K. In: Treatise on Geochemistry, Pergamon, Oxford, 2003.

DeVries, T. and Deutsch, C.: Large-scale variations in the stoichiometry of marine organic matter respiration, Nature Geosci, 7, 890-894, 2014.

35 Duce, R. A., LaRoche, J., Altieri, K., Arrigo, K. R., Baker, A. R., Capone, D. G., Cornell, S., Dentener, F., Galloway, J., Ganeshram, R. S., Geider, R. J., Jickells, T., Kuypers, M. M., Langlois, R., Liss, P. S., Liu, S. M., Middelburg, J. J., Moore, C. M., Nickovic, S., Oschlies, A., Pedersen, T., Prospero, J., Schlitzer, R., Seitzinger, S., Sorensen, L. L., Uematsu, M., Ulloa, O., Voss, M., Ward, B., and Zamora, L.: Impacts of Atmospheric Anthropogenic Nitrogen on the Open Ocean, Science, 320, 893-897, 2008.

40 Durkin, C. A., Estapa, M. L., and Buesseler, K. O.: Observations of carbon export by small sinking particles in the upper mesopelagic, Marine Chemistry, 175, 72-81, 2015.

Engel, A., Szlosek, J., Abramson, L., Liu, Z., and Lee, C.: Investigating the effect of ballasting by CaCO3 in Emiliania huxleyi: I. Formation, settling velocities and physical properties of aggregates, Deep Sea Research Part II: Topical Studies in Oceanography, 56, 1396-1407, 2009.

45 Eppley, R. W. and Peterson, B. J.: Particulate organic matter flux and planktonic new production in the deep ocean, Nature, 282, 677-680, 1979.

Falkowski, P. G., Barber, R. T., and Smetacek, V.: Biogeochemical Controls and Feedbacks on Ocean Primary Production, Science, 281, 200-206, 1998.

Findlater, J.: A major low-level air current near the Indian Ocean during the northern summer, Quart. J. R. Met. Soc., 95, 50 362-380, 1969.

Findlater, J.: A Numerical Index to Monitor the Afro-Asian Monsoon During the Northern Summers, Meteorological Magazine, 106, 170-180, 1977.

France-Lanord, C. and Derry, L. A.: Organic carbon burial forcing of the carbon cycle from Himalayan erosion, Nature, 390, 65-67, 1997.

5   Francois, R., Honjo, S., Krishfield, R., and Manganini, S.: Factors controlling the flux of organic carbon to the bathypelagic zone of the ocean, Global Biogeochemical Cycles, 16, 34-31 - 34-20, 2002.

Galy, V., France-Lanord, C., Beyssac, O., Faure, P., Kudrass, H., and Palhol, F.: Efficient organic carbon burial in the Bengal fan sustained by the Himalayan erosional system, Nature, 450, 407-410, 2007.

Garrison, D. L., Gowing, M. M., and Hughes, M. P.: Nano- and microplankton in the northern Arabian Sea during the
10   Southwest Monsoon, August-September 1995 A US-JGOFS study, Deep Sea Research Part II: Topical Studies in Oceanography, 45, 2269-2299, 1998.

Garrison, D. L., Gowing, M. M., Hughes, M. P., Campbell, L., Caron, D. A., Dennett, M. R., Shalapyonok, A., Olson, R. J., Landry, M. R., and Brown, S. L.: Microbial food web structure in the Arabian Sea: a US JGOFS study, Deep Sea Research II, 47, 1387-1422, 2000.

15   Guidi, L., Stemmann, L., Jackson, G. A., Ibanez, F., Claustre, H., Legendre, L., Picheral, M., and Gorskya, G.: Effects of phytoplankton community on production, size, and export of large aggregates: A world-ocean analysis, Limnology and Oceanography, 54, 1951-1963, 2009.

Gust, G., Byrne, R. H., Bernstein, R. E., Betzer, P. R., and Bowles, W.: Particle fluxes and moving fluids: experience from synchronous trap collections in the Sargasso Sea, Deep Sea Research, 39, 1071-1083, 1992.

20   Gust, G., Michaels, A. F., Johnson, R., Deuser, W. G., and Bowles, W.: Mooring line motions and sediment trap hydromechanics: in situ intercomparison of three common deployment designs, Deep Sea Research I, 41, 831-857, 1994.

Haake, B. and Ittekkot, V.: Die Wind-getriebene "biologische Pumpe" und der Kohlenstoffentzug im Ozean, Naturwissenschaften, 77, 75-79, 1990.

25   Haake, B., Ittekkot, V., Rixen, T., Ramaswamy, V., Nair, R. R., and Curry, W. B.: Seasonality and interannual variability of particle fluxes to the deep Arabian Sea, Deep Sea Research I, 40, 1323-1344, 1993.

Hamm, C. E.: Interactive aggregation and sedimentation of diatoms and clay-sized lithogenic material, Limnology and Oceanography, 47, 1790-1795, 2002.

Heinze, C., Maier-Reimer, E., and Winn, K.: Glacial pCO_2 Reduction by the World Ocean: Experiments with the Hamburg
30   Carbon Cycle Model, Paleoceanography, 6, 395-430, 1991.

Hendiarti, N., Siegel, H., and Ohde, T.: Investigation of different coastal processes in Indonesian water using SeaWiFS data., Deep Sea Research, 51, 85-97, 2004.

Henson, S. A., Sanders, R., Madsen, E., Morris, P. J., Le Moigne, F., and Quartly, G. D.: A reduced estimate of the strength of the ocean's biological carbon pump, Geophysical Research Letters, 38, L04606, 2011.

35   Honjo, S.: Coccoliths: Production, Transportation and Sedimentation, Marine Micropaleontology, 1, 65-79, 1976.

Honjo, S.: Seasonality and Interaction of Biogenic and Lithogenic Particulate Flux at the Panama Basin, Science, 218, 883-884, 1982.

Honjo, S., Dymond, J., Prell, W., and Ittekkot, V.: Monsoon-controlled export fluxes to the interior of the Arabian Sea, Deep Sea Research II, 46, 1859-1902, 1999.

40   Honjo, S., Manganini, S. J., Krishfield, R. A., and Francois, R.: Particulate organic carbon fluxes to the ocean interior and factors controlling the biological pump: A synthesis of global sediment trap programs since 1983, Progress in Oceanography, 76, 217-285, 2008.

Ito, T. and Follows, M. J.: Preformed phosphate, soft tissue pump and atmospheric CO_2, Journal of Marine Research, 63, 813 - 839, 2005.

45   Ittekkot, V.: The abiotically driven biological pump in the ocean and short-term fluctuations in atmospheric CO_2 contents, Global and Planetary Change, 8, 17-25, 1993.

Ittekkot, V. and Haake, B.: The Terrestrial Link in the Removal of Organic Carbon in the Sea. In: Factes of Modern Biogeochemistry, Ittekkot, V., Kempe, S., Michaelis, W., and Spitzy, A. (Eds.), Springer Verlag, Berlin, Heidelberg, New York, 1990.

Ittekkot, V., Nair, R. R., Honjo, S., Ramaswamy, V., Bartsch, M., Manganini, S., and Desai, B. N.: Enhanced particle fluxes in Bay of Bengal induced by injection of fresh water, Nature, 351, 385-387, 1991.

Iversen, M. H., Nowald, N., Ploug, H., Jackson, G. A., and Fischer, G.: High resolution profiles of vertical particulate organic matter export off Cape Blanc, Mauritania: Degradation processes and ballasting effects, Deep Sea Research Part I: Oceanographic Research Papers, 57, 771-784, 2010.

Iversen, M. H. and Ploug, H.: Ballast minerals and the sinking carbon flux in the ocean: carbon-specific respiration rates and sinking velocity of marine snow aggregates, Biogeosciences, 7, 2613-2624, 2010.

Iversen, M. H. and Ploug, H.: Temperature effects on carbon-specific respiration rate and sinking velocity of diatom aggregates – potential implications for deep ocean export processes, Biogeosciences, 10, 4073-4085, 2013.

Iversen, M. H. and Robert, M. L.: Ballasting effects of smectite on aggregate formation and export from a natural plankton community, Marine Chemistry, 175, 18-27, 2015.

Jahnke, R. A.: The global ocean flux of particulate organic carbon: Areal distribution and magnitude, Global Biogeochemical Cycles, 10, 71-88, 1996.

Keeling, C. D. and Whorf, T. P.: Atmospheric CO_2 concentrations (ppmv) derived from in situ air samples collected at Mauna Loa Observatory, Hawaii, Scrips Institution of Oceanography, University of California La Jolla, California USA 92093 - 04444, 2005. 2005.

Keil, R. G. and Hedges, J. I.: Sorption of organic matter to mineral surfaces and the preservation of organic matter in coastal marine sediments, Chemical Geology, 107, 385-388, 1993.

Klaas, C. and Archer, D. E.: Association of sinking organic matter with various types of mineral ballast in the deep sea: Implications for the rain ratio., Global Biogeochemical Cycles, 16, doi:10.1029/2001GB001765, 2002.

Knox, F. and McElroy, M. B.: Changes in atmospheric CO2: Influence of the marine biota at high latitude, Journal of Geophysical Research: Atmospheres, 89, 4629-4637, 1984.

Koning, E., Brummer, G.-J., Van Raaphorst, W., Van Bennekom, J., Helder, W., and Van Iperen, J.: Settling, dissolution and burial of biogenic silica in the sediments off Somalia (northwestern Indian Ocean), Deep Sea Research Part II: Topical Studies in Oceanography, 44, 1341-1360, 1997.

Kranck, K.: Flocculation of Suspended Sediment in the Sea, Nature, 246, 348-350, 1973.

Kumar, D., M., Naqvi, S. W. A., George, M. D., and Jayakumar, A.: A sink for atmospheric carbon dioxide in the northeastern Indian Ocean, Journal of Geophysical Research, 101, 18,121 - 118,125, 1996.

Kwon, E. Y., Primeau, F., and Sarmiento, J. L.: The impact of remineralization depth on the air-sea carbon balance, Nature Geosci, 2, 630-635, 2009.

Lal, D. and Lerman, A.: Size spectra of biogenic particles in ocean water and sediments, Journal of Geophysical Research, 80, 423-430, 1975.

Laufkötter, C., John, J. G., Stock, C. A., and Dunne, J. P.: Temperature and oxygen dependence of the remineralization of organic matter, Global Biogeochemical Cycles, 31, 1038-1050, 2017.

Laws, E. A., Falkowski, P. G., Smith, W. O., Ducklow, H., and McCarthy, J. J.: Temperature effects on export production in the open ocean, Global Biogeochemical Cycles, 14, 1231-1246, 2000.

Le Moigne, F. A. C., Pabortsava, K., Marcinko, C. L. J., Martin, P., and Sanders, R. J.: Where is mineral ballast important for surface export of particulate organic carbon in the ocean?, Geophysical Research Letters, 41, 8460-8468, 2014.

Lee, C., Hedges, J. I., Wakeham, S. G., and Zhu, N.: Effectiveness of various treatments in retarding microbial activity in sediment trap material and their effects on the collection of swimmers, Limnology and Oceanography, 37, 117-130, 1992.

Lee, C., Murray, D. W., Barber, R. T., Buesseler, K. O., Dymond, J., Hedges, J. I., Honjo, S., Manganini, S. J., and Marra, J.: Particulate organic carbon fluxes: compilation of results from the 1995 US JGOFS Arabian Sea Process Study, Deep Sea Research II, 45, 2489-2501, 1998.

Lee, C., Wakeham, S. G., and Arnosti, C.: Particulate organic matter in the sea: the composition conundrum, Ambio, 33, 565-575, 2004.

Logan, B. E. and Hunt, J. R.: Advantages to microbes of growth in permeable aggregates in marine systems1, Limnology and Oceanography, 32, 1034-1048, 1987.

Ludwig, W., Probst, J.-L., and Kempe, S.: Predicting the oceanic input of organic carbon by continental erosion, Global Biogeochemical Cycles, 10, 23-41, 1996.

Luther, M. E. and O'Brien, J. J.: Variability in Upwelling Fields in the Northwestern Indian Ocean - 1. Model Experiments for the Past 18,000 Years, Paleoceanography, 5, 433-445, 1990.

Lutz, M. J., Caldeira, K., Dunbar, R. B., and Behrenfeld, M. J.: Seasonal rhythms of net primary production and particulate organic carbon flux to depth describe the efficiency of biological pump in the global ocean, Journal of Geophysical Research: Oceans, 112, C10011, 2007.

Marsay, C. M., Sanders, R. J., Henson, S. A., Pabortsava, K., Achterberg, E. P., and Lampitt, R. S.: Attenuation of sinking particulate organic carbon flux through the mesopelagic ocean, Proceedings of the National Academy of Sciences of the United States of America, 112, 1089-1094, 2015.

McCave, I. N.: Size Spectra and aggregation of suspended particles in the deep ocean, Deep Sea Research, 31, 329-352, 1984.

McCave, I. N.: Vertical flux of particles in the ocean, Deep Sea Research, 22, 491-502, 1975.

McDonnell, A. M. P., Boyd, P. W., and Buesseler, K. O.: Effects of sinking velocities and microbial respiration rates on the attenuation of particulate carbon fluxes through the mesopelagic zone, Global Biogeochemical Cycles, 29, 175-193, 2015.

Miklasz, K. A. and Denny, M. W.: Diatom sinkings speeds: Improved predictions and insight from a modified Stokes' law, Limnology and Oceanography, 55, 2513-2525, 2010.

Millero, F. J. and Poisson, A.: International one-atmosphere equation of state of seawater, Deep Sea Research Part A. Oceanographic Research Papers, 28, 625-629, 1981.

Milliman, J. D. and Farnsworth, K. L.: River discharge to the coastal ocean, Cambridge University Press, Cambridge, 2011.

Milliman, J. D. and Meade, R. H.: World-Wide Delivery of River Sediment to the Oceans, The Journal of Geology, 91, 1-21, 1983.

Milliman, J. D., Quraishee, G. S., and Beg, M. A. A.: Sediment discharge from the Indus River to the ocean: past, present and future. In: Marine Geology and Oceanography of Arabian Sea and Coastal Pakistan, Haq, B. U. and Milliman, J. D. (Eds.), Van Nostrand Reinhold Company Scientific and Academic Editions, New York, Cincinnati, Stroudsburg, Toronto, London, Melbourne, 1984.

Mohtadi, M., Steinke, S., Groeneveld, J., Fink, H., G., Rixen, T., Hebbeln, D., Donner, B., and Herunadi, B.: Low-latitude control on seasonal and interannual changes in planktonic foraminiferal flux and shell geochemistry off south Java: A sediment trap study, Paleoceanography, 24, PA1201, 2009.

Mottana, A., Crespi, R., and Liborio, G.: Simon & Schuster's guide to rocks & minerals, Simon and Schuster, New York, 1978.

Nair, R. R., Ittekkot, V., Manganini, S. J., Ramaswamy, V., Haake, B., Degens, E. T., Desai, B. N., and Honjo, S.: Increased particle flux to the deep ocean related to monsoons, Nature, 338, 749-751, 1989.

Neil, R.: The Holocene: An Environmental History, Wiley-Blackwell, Hoboken, New Jersey USA, 2014.

Nielsen, E. S.: Measurement of the Production of Organic Matter in the Sea by means of Carbon-14, Nature, 167, 684-685, 1951.

Osipov, V. I.: Density of clay minerals, Soil Mechanics and Foundation Engineering, 48, 231-240, 2012.

Pabortsava, K., Lampitt, R. S., Benson, J., Crowe, C., McLachlan, R., Le Moigne, F. A. C., Mark Moore, C., Pebody, C., Provost, P., Rees, A. P., Tilstone, G. H., and Woodward, E. M. S.: Carbon sequestration in the deep Atlantic enhanced by Saharan dust, Nature Geosci, 10, 189-194, 2017.

Palamenghi, L., Schwenk, T., Spiess, V., and Kudrass, H. R.: Seismostratigraphic analysis with centennial to decadal time resolution of the sediment sink in the Ganges–Brahmaputra subaqueous delta, Continental Shelf Research, 31, 712-730, 2011.

Passow, U. and Carlson, C. A.: The biological pump in a high CO2 world, Marine Ecology Progress Series, 470, 249-271, 2012.

Ploug, H. and Grossart, H.-P.: Bacterial growth and grazing on diatom aggregates: Respiratory carbon turnover as a function of aggregate size and sinking velocity, Limnology and Oceanography, 45, 1467-1475, 2000.

Quillin, M. L. and Matthews, B. W.: Accurate calculation of the density of proteins, Acta Crystallographica Section D, 56, 791-794, 2000.

Ragueneau, O., Schultes, S., Bidle, K., Claquin, P., and Moriceau, B.: Si and C interactions in the world ocean: Importance of ecological processes and implications for the role of diatoms in the biological pump, Global Biogeochemical Cycles, 20, GB4S02, 2006.

Ramage, C. S.: Monsoon Climates. In: The Encyclopedia of Climatology, Oliver, J. E. and Fairbridge, R. W. (Eds.), Van Nostrand Reinhold Company, New York, 1987.

Ramage, C. S.: Monsoon Meteorology, Academic Press, New York, London, 1971.

Ramaswamy, V., Nair, R. R., Manganini, S., Haake, B., and Ittekkot, V.: Lithogenic fluxes to the deep Arabian Sea measured by sediment traps, Deep Sea Research, 38, 169-184, 1991.

Ramaswamy, V., Vijay Kumar, B., Parthiban, G., Ittekkot, V., and Nair, R. R.: Lithogenic fluxes in the Bay of Bengal measured by sediment traps, Deep Sea Research Part I: Oceanographic Research Papers, 44, 793-810, 1997.

Ramesh Kumar, M. R. and Prasad, T. G.: Annual and interannual variation of precipitation over the tropical Indian Ocean, Journal of Geophysical Research, 102, 18,519-518,527, 1997.

Ramesh Kumar, M. R. and Schlüssel, P.: Air-Sea Interaction over the Indian Ocean During the Two Contrasting Monsoon Years 1987 and 1988 Studied with Satellite Data, Theor. Appl. Climatol., 60, 219-231, 1998.

Rao, C. K., Naqvi, S. W. A., Kumar, M. D., Varaprasad, S. J. D., Jayakumar, D. A., George, M. D., and Singbal, S. Y. S.: Hydrochemistry of the Bay of Bengal: possible reasons for a different water-column cycling of carbon and nitrogen from the Arabian Sea, Marine Chemistry, 47, 279-290, 1994.

Rex, R. W. and Goldberg, E. D.: Quartz Contents of Pelagic Sediments of the Pacific Ocean1, Tellus, 10, 153-159, 1958.

Riebesell, U., Schulz, K. G., Bellerby, R. G. J., Botros, M., Fritsche, P., Meyerhofer, M., Neill, C., Nondal, G., Oschlies, A., Wohlers, J., and Zollner, E.: Enhanced biological carbon consumption in a high CO_2 ocean, Nature, 450, 545-548, 2007.

Risien, C. M. and Chelton, D. B.: A Global Climatology of Surface Wind and Wind Stress Fields from Eight Years of QuikSCAT Scatterometer Data, Journal of Physical Oceanography, 38, 2379-2413, 2008.

Rixen, T., Guptha, M. V. S., and Ittekkot, V.: Sedimentation. In: Report of the Indian Ocean Synthesis Group on the Arabian Sea Process Study, Watts, L., Burkill, P. H., and Smith, S. (Eds.), JGOFS International Project Office, Bergen, 2002.

Rixen, T., Haake, B., Ittekkot, V., Guptha, M. V. S., Nair, R. R., and Schlüssel, P.: Coupling between SW monsoon-related surface and deep ocean processes as discerned from continuous particle flux meausurements and correlated satellite data, Journal of Geophysical Research, 101, 28,569-528,582, 1996.

Rixen, T., Ittekkot, V., Herundi, B., Wetzel, P., Maier-Reimer, E., and Gaye-Haake, B.: ENSO-driven carbon see saw in the Indo-Pacific, Journal of Geophysical Research Letters, 33, doi:10.1029/2005GL024965, 2006.

Rixen, T., Ramaswamy, V., Gaye, B., Herunadi, B., Maier-Reimer, E., Bange, H. W., and Ittekkot, V.: Monsoonal and ENSO Impacts on Export Fluxes and the Biological Pump in the Indian Ocean In: Indian Ocean Biogeochemical Processes and Ecological Variability, Hood, R. R., Wiggert, J. D., Naqvi, S. W. A., Smith , S., and Brink , K. (Eds.), 185, AGU, Washington, 2009.

Rochford, D. J.: Source regions of oxygen maxima in intermediate depths of the Arabian Sea, Marine and Freshwater Research, 17, 1-30, 1966.

Romero, O. E., Rixen, T., and Herunadi, B.: Effects of hydrographic and climatic forcing on diatom production and export in the tropical southeastern Indian Ocean, Marine Ecology Progress Series, 384, 69-82, 2009.

Ryther, J. H. and Menzel, D. W.: On the production composition and distribution of organic matter in the Western Arabian Sea, Deep Sea Research, 12, 199-209, 1965.

Sabine, C. L. and Tanhua, T.: Estimation of Anthropogenic CO_2 Inventories in the Ocean, Annual Review of Marine Science, 2, 175-198, 2009.

Sarmiento, J. L. and Gruber, N.: Ocean Biogeochemical Dynamics, Princeton University Press, Princeton New Jersey, 2006.

Sarmiento, J. L. and Toggweiler, J. R.: A new model for the role of the oceans in determining atmospheric pCO_2, Nature, 308, 621-624, 1984.

Sastry, J. S. and D'Souza, R. S.: Upwelling & Upward Mixing in the Arabian Sea, Indian Journal of Marine Sciences, 1, 17-27, 1972.

Schiebel, R.: Planktic foraminiferal sedimentation and the marine calcite budget, Global Biogeochemical Cycles, 16, 13-11 - 13-21, 2002.

Schiebel, R., Barker, S., Lendt, R., Thomas, H., and Bollmann, J.: Planktic foraminiferal dissolution in the twilight zone, Deep Sea Research Part II: Topical Studies in Oceanography, 54, 676-686, 2007.

Schiebel, R. and Hemleben, C.: Interannual variability of planktic foraminiferal populations and test flux in the eastern North Atlantic Ocean (JGOFS), Deep Sea Research Part II: Topical Studies in Oceanography, 47, 1809-1852, 2000.

5 Schiebel, R. and Hemleben, C.: Modern planktic foraminifera, Paläontologische Zeitschrift, 79, 135 - 148, 2005.

Schmidt, K., De La Rocha, C. L., Gallinari, M., and Cortese, G.: Not all calcite ballast is created equal: differing effects of foraminiferan and coccolith calcite on the formation and sinking of aggregates, Biogeosciences, 11, 135-145, 2014.

Schott, F. and McCreary, J. P., Jr.: The monsoon circulation of the Indian Ocean, Progress in Oceanography, 51, 1 - 123, 2001.

10 Sharma, G. S.: Upwelling Off the Soutwest Coast of India, Indian Journal of Marine Sciences, 7, 209-218, 1978.

Shetye, S. R., Gouveia, A. D., Shenoi, S. S. C., Sundar, D., Michael, G. S., Almeida, A. M., and Santanam, K.: Hydrography and circulation off the west coast of India during the Southwest Monsoon 1987, Journal of Marine Research, 48, 359-378, 1990.

Siegel, D. A., Buesseler, K. O., Doney, S. C., Sailley, S. F., Behrenfeld, M. J., and Boyd, P. W.: Global assessment of ocean carbon export by combining satellite observations and food-web models, Global Biogeochemical Cycles, 28, 181-196, 2014.

Siegenthaler, U. and Wenk, T.: Rapid atmospheric CO_2 variations and ocean circulation, Nature, 308, 624-627, 1984.

Sirocko, F., Sarnthein, M., Erlenkeuser, H., Lange, H., Arnold, M., and Duplessy, J. C.: Century-scale events in monsoonal climate over the past 24,000 years, Nature, 364, 322-324, 1993.

20 Smith , S., L.: The Arabian Sea of the 1990s: New Biogeochemical Understanding, Progress In Oceanography, 65, 113 - 290, 2005.

Smith, S. L.: The northwestern Indian Ocean during the monsoons of 1979: distribution, abundance, and feeding of zooplankton, Deep Sea Research, 29, 1331-1353, 1982.

Smith, T. M., Reynolds, R. W., Peterson, T. C., and Lawrimore, J.: Improvements to NOAA's historival merged land-ocean surface temperature analysis (1880 - 2006), Journal of Climate, 21, 2283 - 2296, 2008.

Subramanian, V., Richey, J. E., and Abbas, N.: Geochemistry of River Basins of India Part II - Preliminary Studies on the Particulate C and N in the Ganges-Brahmaputra River System, Mitt. Geol.-Paläont. Inst. Univ. Hamburg, 58, 513-518, 1985.

Susanto, R. D., Gordon, A. L., and Zengh, Q.: Upwelling along the coasts of Java and Sumatra and its relation to ENSO, Journal of Marine Research Letters, 28, 1599-1602, 2001.

Syvitski, J. P. M., Vörösmarty, C. J., A.J., K., and Green, P.: Impact of humans on the flux of terrestrial sediment to the global ocean, Science, 308, 376 - 380, 2005.

Tchernia, P.: Descriptive regional oceanography, Oxford Pergamon Press, Oxford, UK, 1980.

Tegen, I. and Fung, I.: Contribution to the atmospheric mineral aerosol load from land surface modification, Journal of Geophysical Research, 100, 18,707-718,726, 1995.

Turner, J. T.: Zooplankton fecal pellets, marine snow, phytodetritus and the ocean's biological pump, Progress in Oceanography, 130, 205-248, 2015.

Unger, D., Ittekkot, V., Schäfer, P., and Tiemann, J.: Biogeochemistry of particulate organic matter from the Bay of Bengal as discernible from hydrolysable neutral carbohydrates and amino acids, Marine Chemistry, 96, 155-184, 2005.

40 Unger, D., Ittekkot, V., Schafer, P., Tiemann, J., and Reschke, S.: Seasonality and interannual variability of particle fluxes to the deep Bay of Bengal: influence of riverine input and oceanographic processes, Deep Sea Research Part II: Topical Studies in Oceanography, 50, 897-923, 2003.

Volk, T. and Hoffert, M. I.: The carbon cycle and atmospheric CO_2, natural variation archean to present. In: The Carbon Cycle and Atmospheric CO_2: Natural Variations Archean to Present, Sundquist, E. T. and Broecker, W. S. (Eds.), AGU, Washington, 1985.

45

Wagner, W. and Pruß, A.: The IAPWS Formulation 1995 for the Thermodynamic Properties of Ordinary Water Substance for General and Scientific Use, Journal of Physical and Chemical Reference Data, 31, 387-535, 2002.

Westberry, T. K., Williams, P. J. l. B., and Behrenfeld, M. J.: Global net community production and the putative net heterotrophy of the oligotrophic oceans, Global Biogeochemical Cycles, 26, GB4019, 2012.

Wiggert, J. D., Murtugudde, R. G., and Christian, J. R.: Annual ecosystem variability in the tropical Indian Ocean: Results of a coupled bio-physical ocean general circulation model, Deep Sea Research Part II: Topical Studies in Oceanography, 53, 644-676, 2006.

5   Wilson, J. D., Barker, S., and Ridgwell, A.: Assessment of the spatial variability in particulate organic matter and mineral sinking fluxes in the ocean interior: Implications for the ballast hypothesis, Global Biogeochemical Cycles, 26, GB4011, 2012.

Winter, A. and Siesser, W. G.: Coccolithophores, Cambridge University Press, New York, 1994.

Captions

10   **Figure 1: Bathymetric chart of the northern Indian Ocean and the adjacent land mass. Data were obtained from http://Ingrid.ldgo. Columbia.edu/SOURCE/WORLDBATH. White circles show the sediment trap sites operated by the joint Indo/German and Indonesian German projects (see Tab. 1). The black circles and diamonds represent the US JGOFS sediment trap site M1 to M5 (Honjo et al., 1999; Lee et al., 1998) and the Dutch sediment trap sites in the Arabian Sea and off Somalia (Koning et al., 1997).**

15   **Figure 2. Monthly mean wind speeds (a, b), derived from the Scatterometer Climatology of Ocean Winds (Risien and Chelton, 2008) indicating the Findlater Jet during the summer monsoon (August) in the Arabian Sea. Monthly mean sea surface salinities (c, d) derived from the Soil Moisture and Ocean Salinity (SMOS) satellite mission. The SMOS-data covering the period between 2010 and 2012 were smoothed and downloaded from ftp://ftp.icdc.zmaw.de/smos_sss/. Monthly mean primary production rates (Behrenfeld and Falkowski, 1997) covering the periods between 2002 and 2014 (e, f). The black circles show the sediment trap sites**
20   **(Fig. 1, Tab. 1).**

Figure 3: Monthly mean sea surface temperature in the Indian Ocean (Smith et al., 2008) and the surface ocean circulation simplified and redrawn for Schott and McCreary (2001). The arrows indicate the South Equatorial Current (SEC), South Monsoon Current (SMC), Sri Lanka Dome (SD), East Indian Coastal Current (EICC), South Java Current (SJC), Indonesian Through Flow (ITF), Somali Current (SC), Great Whirl (GW), Ras al Had Jet (RHJ), West Indian Coastal Current (WICC),
25   **North Monsoon Current (NMC). The black circles show the sediment trap sites (Fig. 1, Tab. 1).**

Figure 4: Monthly mean organic carbon fluxes (POC) obtained from our sediment trap experiments in the Arabian Sea (a) and the Bay of Bengal (c) as well as monthly mean primary production rates (Behrenfeld and Falkowski, 1997) selected for the sediment trap sites (b, d). The sediment trap data were normalized to a water depth of 2000 m by using the equation introduced by Rixen et al. (2002).

30   **Figure 5: Organics carbon fluxes measure at JAM and the primary production rates selected for the JAM site.**

Figure 6. Primary production versus the ratio between export production derived from Eq.3 (H-Export) and Eq.1 (E-Export) whereas a SST of 28.5 (red line) and 26.5 °C (blue line) was considered to calculate export production by using Eq.3. Due to the multiplication with 100 the ratio represents the share of the H-Export to the E-Export. The circles show the data obtained from the trap sites. Their increase at higher primary production rates are caused by upwelling and deep mixing which lower SST and
35   **increase primary productions.**

Figure 7: (a) The proportion of the exported organic carbon, which reaches the deep sea (black) and the respective respiration of organic matter in the water column during the summer, winter and inter-monsoon seasons at our trap sites (red). The open circles indicate the Arabian Sea data. (b) Excess organic carbon fluxes (POC$_{Excess}$) versus the lithogenic matter content. The open circles indicate data obtained at WAST and SBBT during the upwelling season in summer. This two data points were excluded from the
40   **regression analysis. (c) Excess organic carbon fluxes (POC$_{Excess}$) versus carbonate flux. Open circle indicate data from the northern and central Bay of Bengal as well as from the Sea off South Java. These data were also excluded from the regression analysis.**

Figure 8: The organic carbon fluxes (POC) versus the lithogenic matter content (a) and carbonate flux (b). The red circle indicate trap sites influenced by upwelling in the Arabian Sea and the southern Bay of Bengal (SBBT), the black circles show the data from the river-dominated regions in the Bay of Bengal and off South Java. The error bars indicate interannual variability and arrows
45   **hint to the assumed main forcing mechanism.**

Figure 9: Densities of bulk components including quarz and illite as representatives of lithogenic matter (red lines, and circle). Black circles and lines indicate the densities of crystalline analogues and of cellulose as an example of a carbohydrate. The data were compiled from the literature and the references are given in the text. The grey area shows the density range of sea water.

Figure 10: (a) Annual mean lithogenic matter content at the trap sites in the Indian Ocean versus sinking speeds derived from the density of the solids (Eqs. 6 - 9) including the regression equation and line. The red circle indicates sinking speeds derived from the US JGOFS sediment trap sites in the western Arabian Sea (Berelson, 2001) and the blue circle represents sinking speeds derived from the density of the solids by setting the lithogenic matter flux to zero. The carbonate and biogenic opal ratio causes the variability which the error bar indicates. (b) Annual mean organic carbon fluxes determined at the sediment trap sites versus organic carbon fluxes calculated by using Eq.10 and sinking speed shown in figure 10 a. The export production was derived from Eq.1 (red circles), 2 (blue circles), and 3 (black circles). The red colure shows the regression equation and line obtained from the correlation between the calculated and measured fluxes whereas the respective export production used to calculate the organic carbon flux was derived from Eq.1. The black line indicates the 1:1 line in b and c. (c) Calculated versus measured fluxes as in (b) but the modified Eq.3 was used to calculate the required export production. The errors bars indicate the interannual variability of the measured fluxes and the range caused the variability of the sinking speeds used to calculate the organic carbon flux.

Figure 11. Results obtained from the box model: The atmospheric pCO_2 (a) the organic carbon flux into the deep sea (b), the export production (c) and the total dissolved inorganic carbon (DIC) and phosphate concentrations in the deep sea versus time. Number I shows the results derived from the standard run. Numbers II to III indicate results obtained from the experiments in which the fraction of the export production, which reaches the deep sea from was increased form to 10% to 50% and decreased from 50% to 1 %. During experiment IV, the fraction of export production, which is reaches the deep sea was again set to 10% but in contrast to the former experiments the total phosphate in the surface box was converted in the organic matter and exported. In order to obtain a smooth transition from the standard condition to experiment IV, the increase of the export production was limited to a maximum of 25 Pg C year^{-1} during the transition phase.

Figure 12. The same as figure 11 but the experimental conditions of experiment IV were set as standard. During the model run we again increased and decreased, respectively the fraction of the export production which reaches the deep sea from to 10% to 50% and from 50% to 1 % until towards end the fraction was reset to 10%.

Table 1. Number of station, trap ID, station name, position, water-depth, and trap depth.

No.	Trap ID	Name	Lat.	Lon.	W-Depth	T-Depth
			[°N]	[°N]	[m]	[m]
1	WAST	Western Arabian Sea Trap Station	16.26	60.58	4032	3017
2	CAST	Central Arabian Sea Trap Station	14.51	64.72	3920	2944
3	EAST	Eastern Arabian Sea Trap Station	15.57	68.73	3791	2870
4	NAST	Northern Arabian Sea Trap Station	19.98	65.73	3147	2478
5	EPT	East Pakistan Trap Station	24.77	65.82	1093	590
6	WPT	West Pakistan Trap Station	24.60	65.59	1900	1466
7	NEAST	Northeastern Arabian Sea Trap Station	16.93	67.84	3545	3039
8	SAST	Southern Arabian Sea Trap Station	11.60	66.08	4243	3032
9	EIOT	Equatorial Indian Ocean Trap Station	3.56	77.78	3400	2374
10	NBBT-N	Northern Bay of Bengal Trap Station – North	17.42	89.65	2267	1889
11	NBBT-S	Northern Bay of Bengal Trap Station – South	15.48	89.45	2709	2172
12	CBBT-N	Central Bay of Bengal Trap Station – North	13.14	84.41	3266	2261
13	CBBT-S	Central Bay of Bengal Trap Station – South	11.03	84.43	3462	2527
14	SBBT	Southern Bay of Bengal Trap Station	5.09	87.26	3995	2976
15	JAM	Java Mooring	-8.28	108.02	3250	2456

Table 2. Annual mean total fluxes measured at the trap sites during the years from 1986 to 2003 in the g C m^{-2} year^{-1} including the mean and the standard deviation as well as the number of years (no) in which particle fluxes were measured for more than 150 days year^{-1}.

Trap ID	86	87	88	89	90	91	92	93	94	95	96	97	98	1	2	3	Mean	Std.	No.
									[g C m^{-2} year^{-1}]									[%]	
WAST	45.0	43.0	53.6		66.0	50.6	48.5		52.9	58.6		69.2					54.1	16.6	9
CAST	34.8	34.4	40.7					35.0	40.3		40.0						37.5	8.2	6
EAST	37.4	35.4	34.4	39.0	34.8	37.5		23.3	39.3			34.8					35.1	13.7	9
SAST								43.7									43.7		1
EIOT									35.0	21.3	26.9						27.7	24.7	3
NBBT-N			53.2	50.2					53.4	44.9	47.5	38.9	46.1				47.7	10.7	7
NBBT-S						33.4	34.0										33.7	1.3	2
CBBT-N			43.5	56.7	66.4	60.7		44.8									54.4	18.3	5
CBBT-S							34.8										34.8		1
SBBT			39.9			37.3	35.5	37.2	42.3	47.0	40.5	39.6					39.9	9.0	8
JAM														101.8	122.1	201.2	141.7	37.0	3

Table 3. Trap ID, annual mean bulk fluxes including standard deviation (std) and contents. The standard deviation indicates the interannual variability.

Trap ID	POC	std	Carb.	std	Opal	std	Lith.	std	POC	Carb.	Opal	Lith.
				[g m-2 year-1]						[%]		
WAST	3.1	0.4	29.0	3.5	13.1	3.9	7.9	1.5	5.6	52.3	23.5	14.2
CAST	2.3	0.2	22.4	1.3	4.8	0.4	5.9	0.8	6.1	60.1	12.9	15.9
EAST	2.1	0.3	17.9	2.1	5.4	1.1	7.3	1.1	6.1	52.2	15.8	21.1
EPT	11.9	0.0	62.7	0.0	33.4	0.0	326.2	0.0	2.7	14.1	7.5	73.5
SAST	2.3	0.0	27.1	0.0	6.0	0.0	6.5	0.0	5.2	62.0	13.6	15.0
EIOT	1.5	0.3	16.4	3.1	5.2	1.3	3.6	0.9	5.4	58.7	18.7	12.8
NBBT-N	2.9	0.3	13.3	1.9	10.4	0.7	18.8	3.9	6.1	27.9	21.8	39.5
NBBT-S	2.2	0.0	11.0	0.4	7.7	0.4	11.1	0.3	6.5	32.5	22.9	32.9
CBBT-N	2.9	0.3	15.5	1.0	11.7	2.3	21.9	5.9	5.3	28.5	21.6	40.3
CBBT-S	2.0	0.0	13.4	0.0	8.9	0.0	9.0	0.0	5.7	38.4	25.6	25.7
SBBT	2.3	0.3	20.0	1.8	9.8	1.5	6.1	1.4	5.6	50.0	24.6	15.3
JAM	4.8	0.6	15.1	2.5	31.3	15.6	86.6	23.9	3.4	10.7	22.1	61.1

Table 4. Values used to calculate sinking speeds (Eqs.6 - 9). Densities of the bulk components were obtained from the literature. See Chapter 4.4 for further details.

	Value	Unit
Temperature	10	°C
Salinity	35	
λ	0.12	day^{-1}
Porosity	0.917	
Radius	0.15	mm
Density		
OM		g cm^{-3}
Opal	0.90 ±0.20	g cm^{-3}
Carb.	1.73 ±0.27	g cm^{-3}
Lith.	1.63 ±0.08	g cm^{-3}
	2.70 ±0.05	g cm^{-3}

Table 5 Carrying coefficients derived from the MLR applied to data measured at the trap site
the mean. 'No.' indicates the number of data used for the analysis. (A-Traps) shows the carryi
by applying the MLR to the annual mean sediment trap data.

Trap ID	CaCO$_3$	Std.	P val.	Opal	Std.	P val.	Lith.	Std.	P val.	r^2	No.
WAST	0.044	0.007	0.000	0.046	0.007	0.000	0.132	0.018	0.000	0.958	142
CAST	0.018	0.007	0.008	0.198	0.032	0.000	0.120	0.026	0.000	0.955	88
EAST	0.033	0.007	0.000	0.124	0.020	0.000	0.108	0.014	0.000	0.970	115
SAST	0.011	0.004	0.034	0.049	0.028	0.111	0.256	0.029	0.000	0.998	13
EIOT	0.031	0.008	0.000	0.035	0.034	0.303	0.227	0.029	0.000	0.963	39
NBBT-N	0.090	0.011	0.000	0.070	0.015	0.000	0.046	0.005	0.000	0.973	88
NBBT-S	-0.022	0.031	0.480	0.139	0.048	0.008	0.126	0.023	0.000	0.964	26
CBBT-N	0.096	0.008	0.000	0.057	0.012	0.000	0.033	0.005	0.000	0.972	78
CBBT-S	0.017	0.019	0.372	0.078	0.025	0.011	0.115	0.028	0.002	0.982	13
SBBT	0.041	0.006	0.000	0.073	0.011	0.000	0.115	0.014	0.000	0.960	99
JAM	0.128	0.026	0.000	0.034	0.013	0.010	0.022	0.005	0.000	0.943	54
mean	0.044	0.012		0.082	0.022		0.118	0.018			
A-Traps	0.067	0.018	0.006	0.113	0.062	0.105	0.006	0.021	0.761	0.983	11

Table 6 Contribution of the individual ballast minerals to the predicted POC flux (RIB see Eq. 5

Trap	CaCO$_3$	Opal	Lith.
WAST	47.0	17.8	35.1
CAST	21.1	46.2	32.7
EAST	31.0	30.9	38.1
SAST	13.4	12.8	73.8
EIOT	37.0	11.8	51.2
NBBT-N	42.8	24.5	32.7
NBBT-S	-11.9	51.6	60.4
CBBT-N	55.2	21.4	23.4
CBBT-S	12.0	34.7	53.2
SBBT	36.0	30.9	33.1
JAM	41.1	19.1	39.7
mean	29.5	27.4	43.0
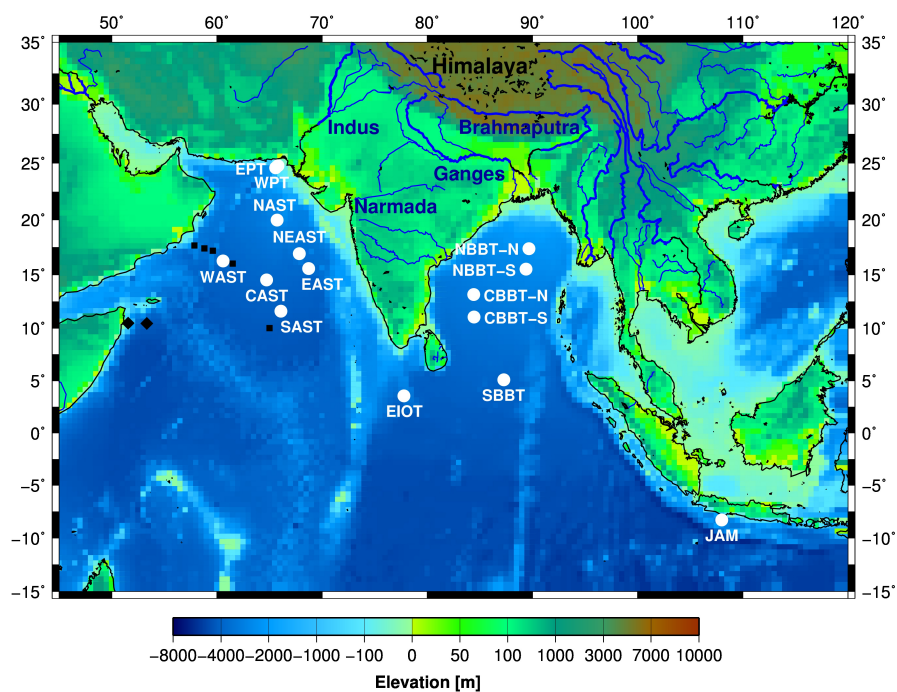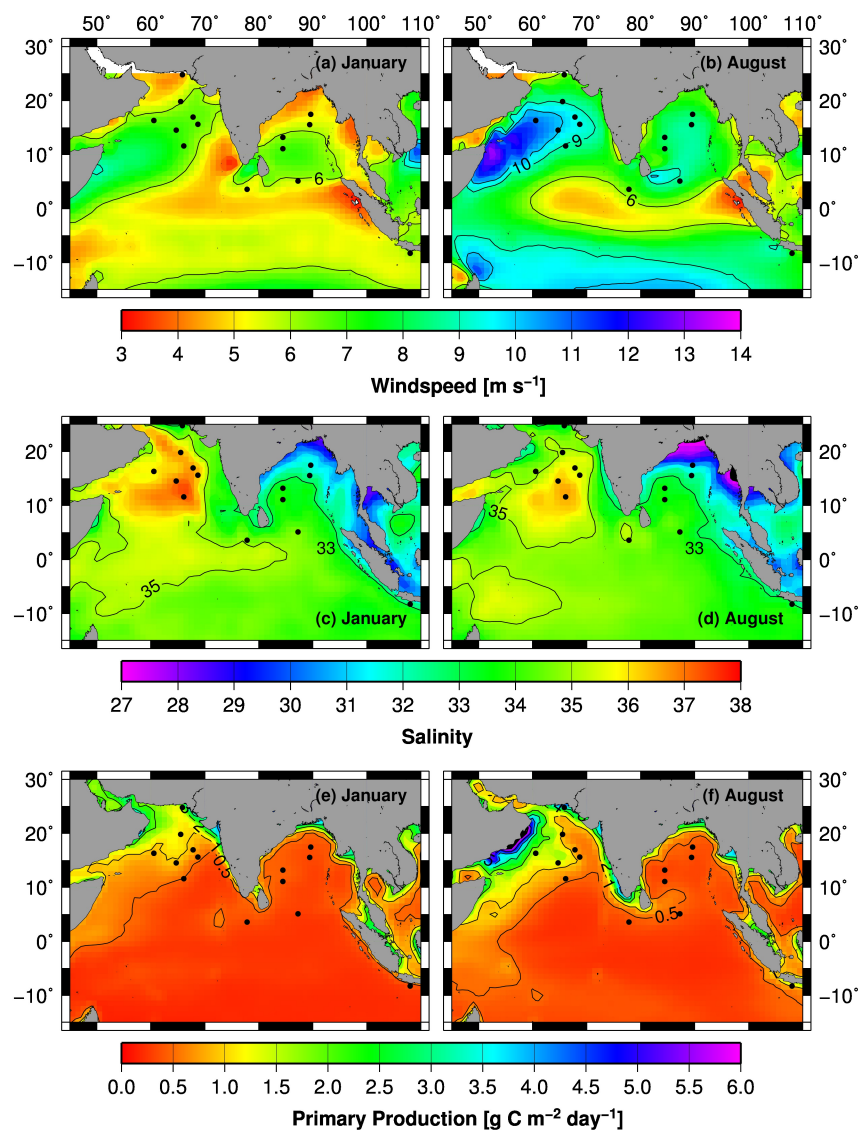
Figure 1
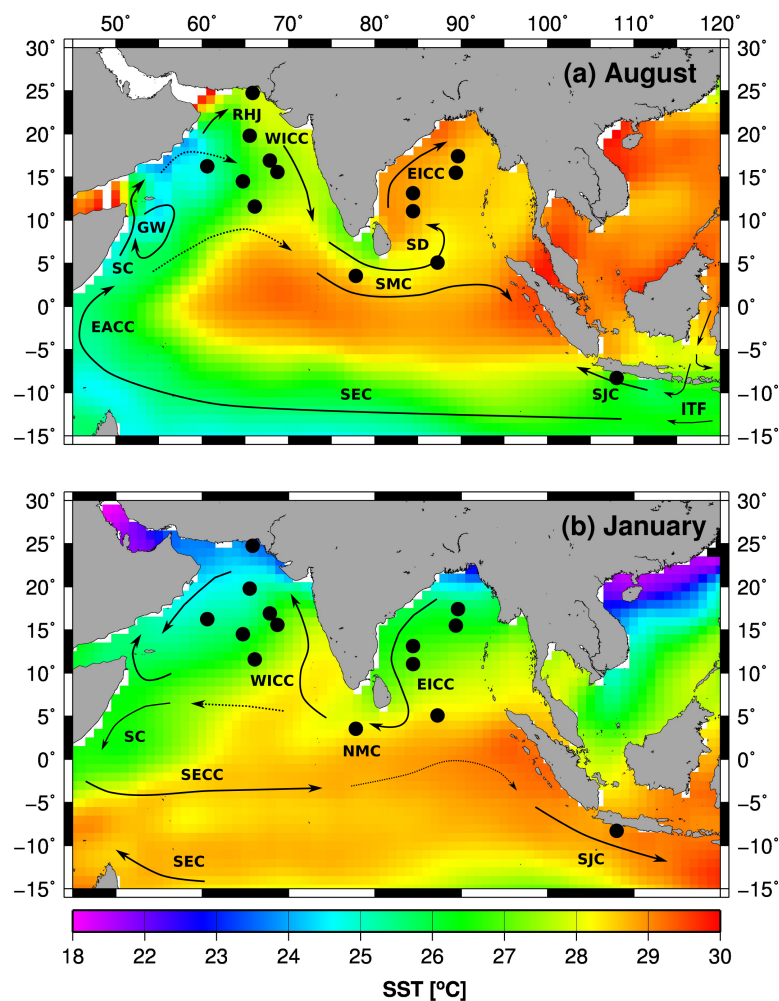
Figure 2

Figure 3

Figure 4
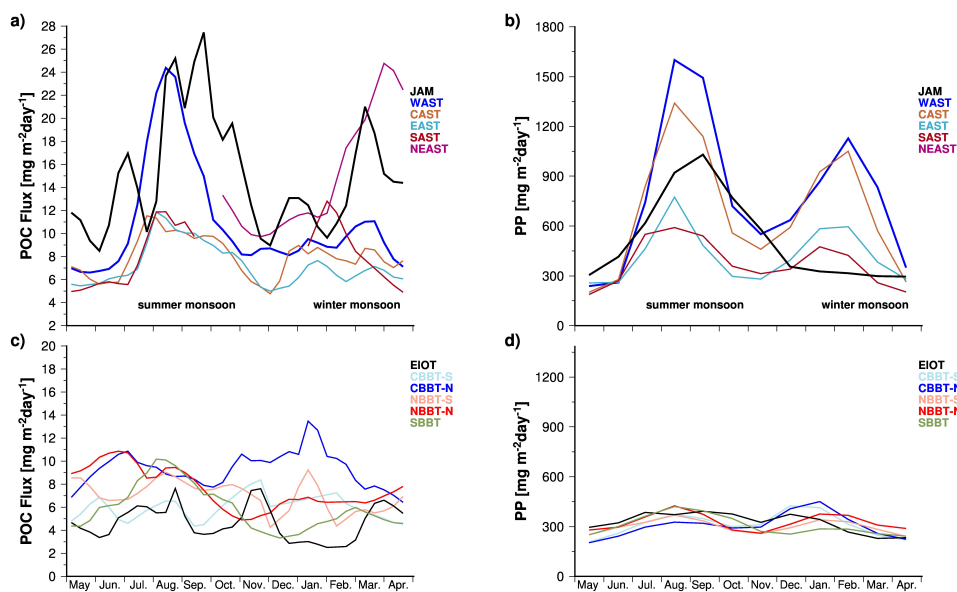
Figure 5
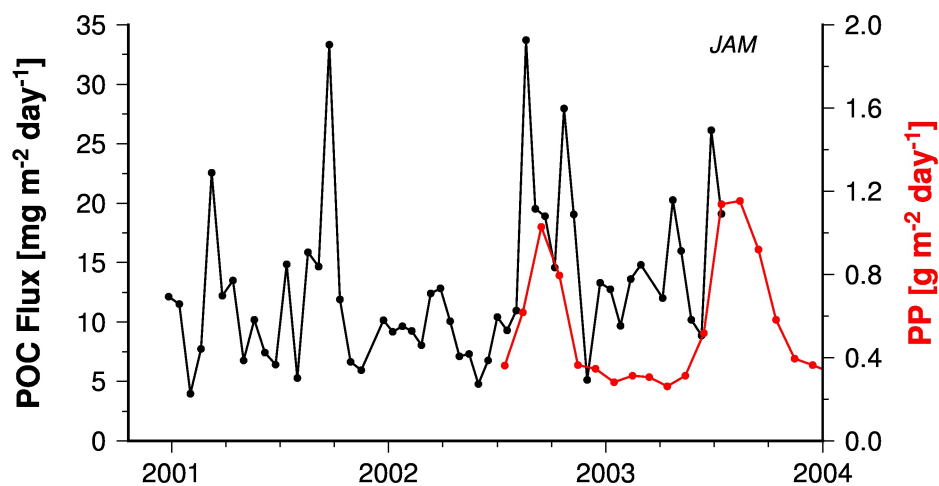
Figure 6
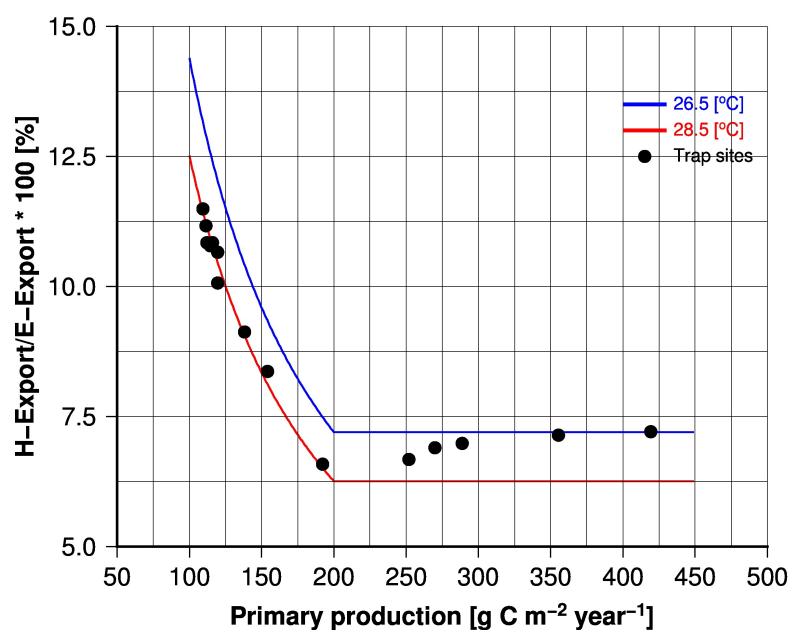
Figure 7
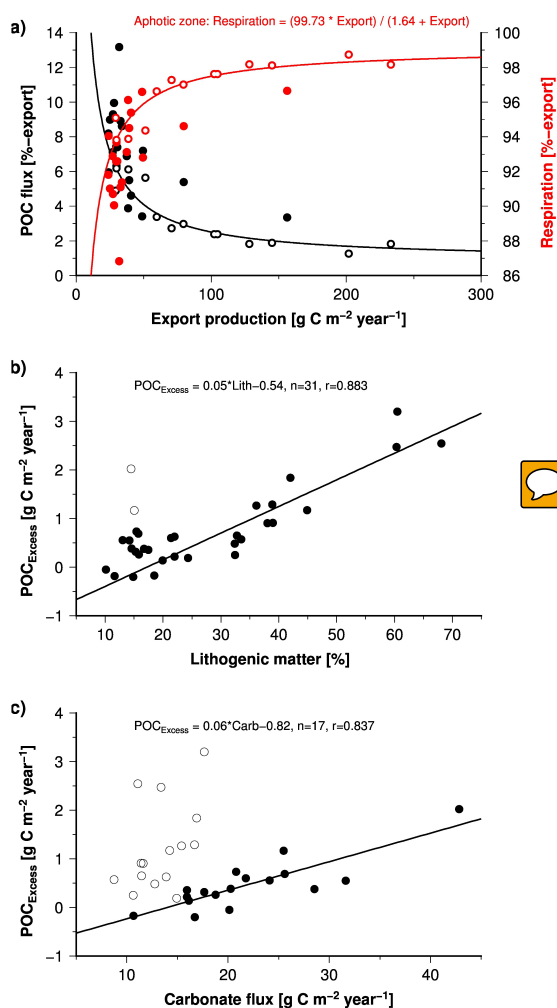
Figure 8
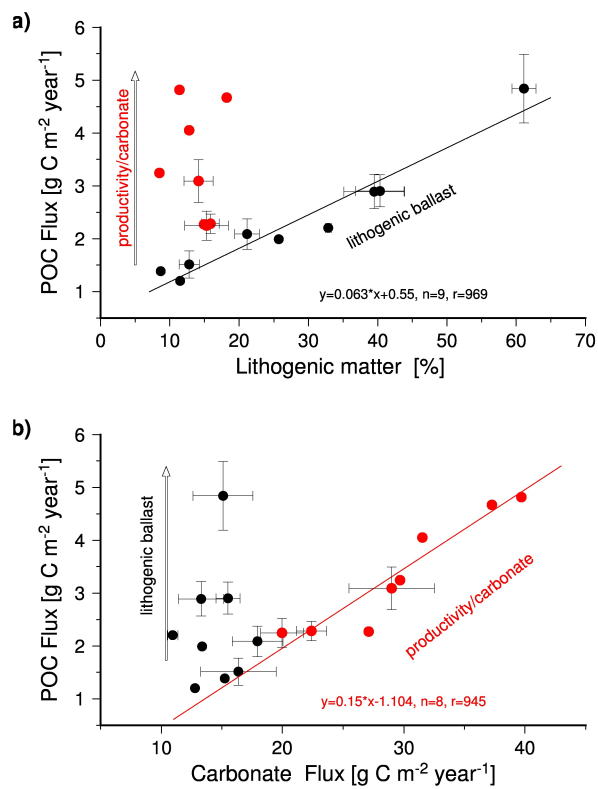
Figure 9
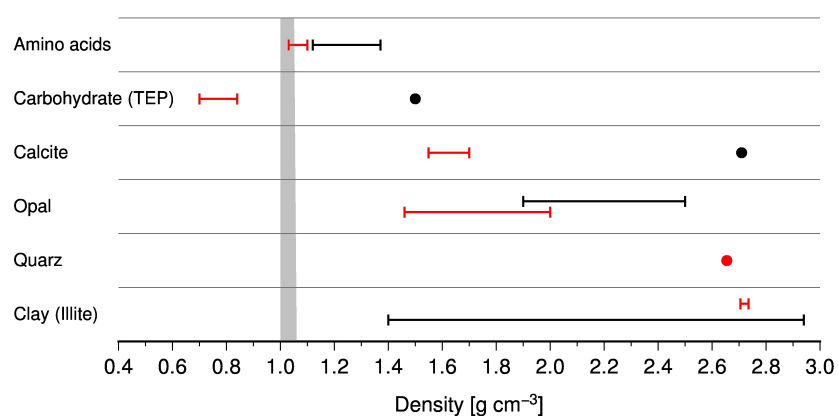
Figure 10

Figure 11

Figure 12